The United Nations University

GEOTHERMAL TRAINING PROGRAMME
Orkustofnun, Grensásvegur 9,
IS-108 Reykjavík, Iceland

Reports 1995
Number 13

ANHYDRITE DEPOSITION IN CAWAYAN WELLS, BACMAN GEOTHERMAL FIELD, PHILIPPINES: PREDICTION AND POSSIBLE REMEDIES

Fidel S. See
Geothermal Division, Geoscientific Dept.,
PNOC-Energy Development Corporation,
PNPC Complex, Merritt Road, Ft. Bonifacio,
Makati, Metro Manila,
PHILIPPINES

ABSTRACT

The anhydrite mineral deposition inside the wellbores of Cawayan wells is investigated in order to predict its occurrence and come up with possible remedies. The chemistry of the fluids is thoroughly evaluated and some geochemical indicators of deposition such as Ca^{2+}, SO_4^{2-}, Mg^{2+}, SiO_2, and Cl^- are established. The behaviour of various calcium and sulphate species during deposition, and the effects of temperature and pH are determined using the SOLVEQ and WATCH 2.1 chemical speciation programmes. Results show that with increasing temperature, the activity of sulphate and calcium species in solution decreases and consequently anhydrite supersaturation is increased. At low pH, sulphate activity is significantly reduced by the formation of bisulphate ions, and anhydrite undersaturation is attained; at high pH, undersaturation is also predicted because of decrease in calcium activity. However, the solution becomes supersaturated with respect to calcite at high pH. The CHILLER programme is utilized to simulate fluid-fluid mixing, and determine the effects of NaCl addition, Na_2HPO_4 addition, acid treatment, and $CaCl_2$ injection on anhydrite deposition. Results show that NaCl, Na_2HPO_4 and HCl are possible inhibitors of anhydrite deposition. Increasing the salinity of production fluid before mixing with high-sulphate waters tends to retard deposition and increase the amount of mixing fluid necessary to initiate formation of anhydrite. Na_2HPO_4 prevents anhydrite deposition by significantly reducing activity of calcium through association with phosphate ions. However, the solution tends to become supersaturated with respect to apatite, which may be deposited. $CaCl_2$ addition can induce deposition in acid zones and thus seal them off but this further lowers the pH of the high-sulphate acid fluid as bisulphate dissociates into sulphate ions and releases hydrogen ions.

1. INTRODUCTION

The Bacman geothermal production field is located on the southern tip of the Bicol peninsula in the Philippines. A 110 MW_e geothermal power plant in the Palayan Bayan sector, and a 20 MW_e modular plant in the Cawayan sector have been fully operational since 1994. A second 20 MW_e plant is currently under development in the Botong sector (Figure 1).

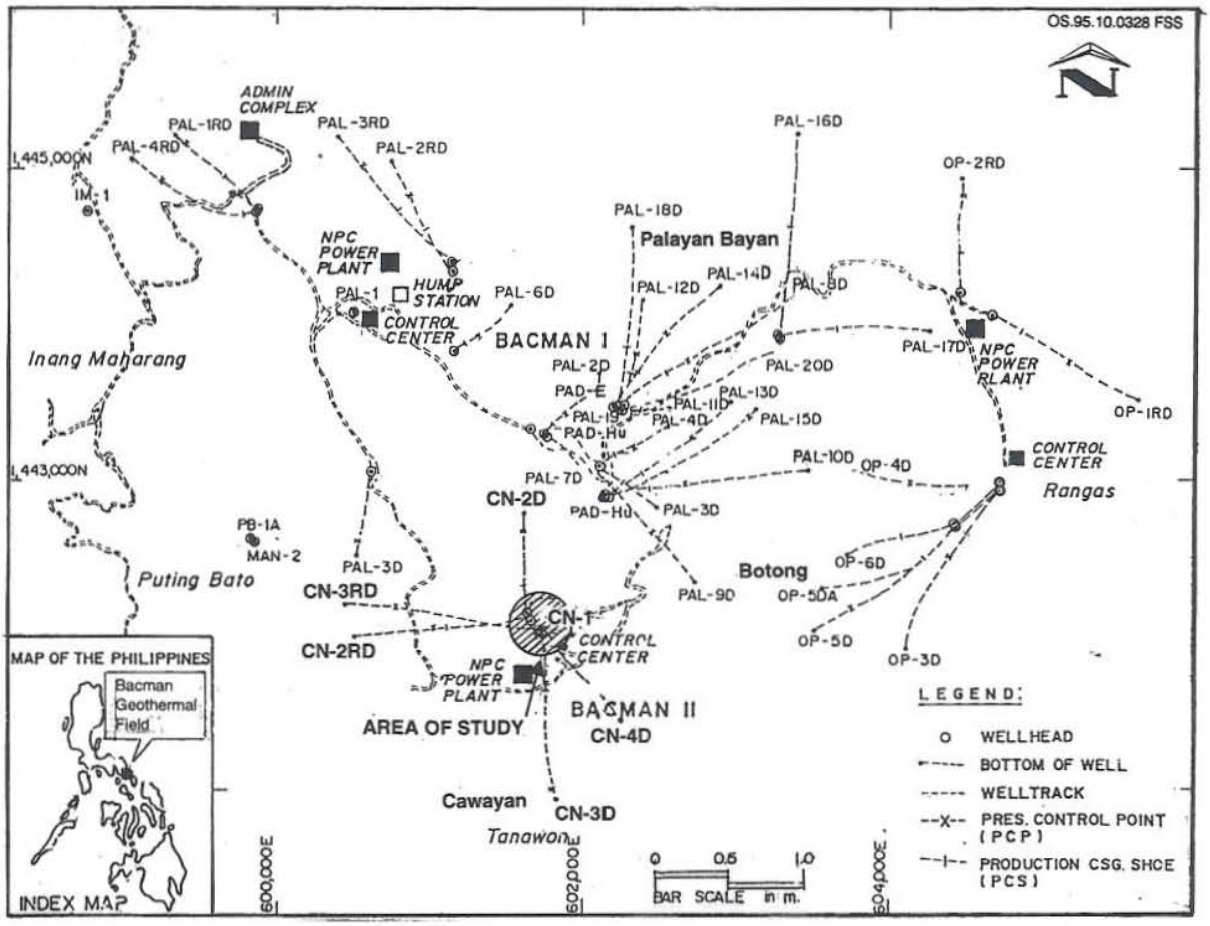

FIGURE 1: Location map of Bacman geothermal field and well targets

The Cawayan sector is initially composed of two production wells, each with an output of about 10 MW_e. Less than a year after commissioning, problems associated with corrosion and mineral deposition inside the wellbores started to significantly decrease the output of the two wells. Petrological analyses of the mineral deposits yielded mostly anhydrite, with small amounts of pyrite, opaques, and corrosion products. Work-over operations using drilling rigs were conducted to mechanically clean the boreholes. The improvement after cleaning was however only temporary and after a few months, deposition started to clog the wells again. Subsequently two additional wells were drilled to maintain the 20 MW_e production of the field. Mitigating measures undertaken (Fragata, 1994) in the new wells are deepening the production casing shoes, casing-off and cementing acid zones, and using corrosion-resistant casings. Calcium chloride injection in the acid zones is also practised during drilling.

Despite the preventive measures implemented, the possibility of anhydrite and other mineral deposition during long-term production cannot be totally eliminated. The original wells are still hampered by anhydrite deposition and regular cleaning by drilling rigs is very costly. Therefore a more thorough understanding of the deposition process, an efficient and reliable method of monitoring, and an investigation of possible methods of deposition control, are necessary.

The aim of this report is to determine the anhydrite saturation conditions of the Cawayan fluids; establish some geochemical indicators of anhydrite deposition; characterize speciation and mineral-solution

equilibria of the fluids responsible for the deposition; simulate saturation conditions at different temperatures, pH, salinity, and mixing proportions; and investigate possible chemical methods of control through simulations.

2. BACKGROUND

2.1 Geology and hydrothermal alteration

The Cawayan wells penetrated the so-called Pocdol volcanic formation, one of the lithologic units of the Bacman geothermal field. This formation is composed of moderately to intensely and completely altered volcanic rocks of andesite lavas, tuffs, and breccia (PNOC-EDC, 1989). This is dissected by the Gayong sedimentary formation in the Botong and Palayan Bayan sectors, and by several andesitic and microdioritic dykes called the Cawayan intrusive complex (PNOC-EDC, 1989). All the Cawayan wells, except CN-3D intersected the Cawayan intrusive complex (Fragata, 1991). The hydrothermal alteration encountered in the wells is generally neutral. These consist of quartz, calcite, anhydrite, epidote, illite, smectite, actinolite, biotite, chlorite, clinozoisite, pyrite, hematite, magnetite, and goethite (Ramos, 1991). Acid alteration products consisting of kaolinite, dickite, alunite, and pyrophyllite, are also abundant; sulphur crystals have been observed megascopically in well CN-2RD at 100-415 mMD (measured depth) (Ramos, 1991). Acid alteration is usually observed at shallower depths, above 1000 mVD (vertical depth), but has also been detected at deeper levels such as diaspore at 1710 mVD in well CN-2RD (Ramos, 1991).

2.2 Fluid chemistry

The chemistry of the Cawayan fluids has been discussed thoroughly in several PNOC-EDC internal reports (e.g. KRTA, 1985; Solis, 1988; See, 1991). There are generally two types of thermal fluids in the sector. First the dominant fluid which is the hotter and deeper, neutral geothermal production brine; and the second one is the colder, shallower, high-sulphate and usually acidic fluid. Particular interest has been devoted to the occurrence and origin of the acid fluids in the area.

The production fluids are neutral geothermal brines with baseline sulphate concentrations of 19 to 29 mg/kg, and calcium concentrations of 138 to 175 mg/kg in weirbox and Webre separator samples. The weirbox samples are collected at atmospheric pressure while Webre samples are collected at 5 to 8.5 bars absolute. The fluids are relatively saline with chloride concentrations of approximately 7000 to 8000 mg/kg and ionic strength of about 0.2 in water phase. pH measured at 25°C ranges from 7.05 to 7.83. Quartz and measured temperatures range from 270 to 275°C.

In contrast the acid fluids have been found to be more dilute, colder, and contain enormous amounts of sulphate ranging from 381 to 1630 mg/kg. pH measured at 25°C ranges from 2.6 to 5.1. Calcium concentration is relatively low ranging from 6 to 89 mg/kg. Chloride concentrations vary from 142 to 5000 mg/kg, and the ionic strength is less than 0.1. Silica quartz geothermometer and measured temperatures range from 230°C to approximately 260°C. These fluids are also characterized by high iron and magnesium contents. In Cawayan production wells, these types of fluid are normally found in the shallower zones, from about 1000 mVD and above. However, in reinjection wells such as CN-2RD and CN-3RD, high-sulphate fluids exist at depth. Representative chemical data used in this study are presented in Tables 1 and 2.

TABLE 1: Cawayan representative baseline well discharge and downhole chemistry

Discharged samples (collected at weirbox and using Webre separator)																					
Well	Date	BPP	WHP	Hd	TMF	SP	pH	Concentration in mg/kg *												mmole/ 100moles**	
			Mpaa	kJ/kg	kg/s	MPaa	25°C	Na	K	Ca	Mg	Fe	Cl	SO_4	H_2S	HCO_3	TCO_2	B	SiO_2	CO_2	H_2S
CN-1	09-12-81	A2	2.34	1220	38.3	0.094	7.78	4654	926	175	0.15		8757	23		10.7			873	229	6.92
CN-1	09-24-81	B1	2.43	1545	24.7	0.094	7.83	4784	950	169	0.13		8757	29		3.1		37	854	166	5.3
CN-1	09-29-81	FBD	0.84	1267	101.2	0.094	7.73	4691	898	177	0.19		8686	26		7		36	865	175	5.25
CN-1	11-19-82	B4	0.09	1214	13	0.094	7.71	4542	921	174	0.06	0.23	8693	22		2.3		37	806	191	7.07
CN-2D	10-13-82	FBD	0.54	1174		0.507	3.83	2438	228	9	12.7	145	3425	1230	0.68			20	503	14844	54.6
CN-2D	10-20-82	FBD	0.53	1120		0.094	3.82	3111	291	13	16.2	179	4343	1610	0.35	150		23	608	16438	62.6
CN2RD	05-10-91	FBD	0.51	965	25.1	0.094	3.74	455	46	17	8.2	4.25	206	871				5	638	419	16.1
CN-3D	10-11-90	FBD	-	1232		0.728	7.24	4215	865	174	0.13	0.19	7768	25	2.52	13.4	12.3	41	741		
CN-3D	10-16-90	A1	2.44	1108		0.715	7.28	4215	899	171	1.39	1.08	7811	18		9.4	9.9	40	740	233	10.9
CN-3D	10-20-90	A3	2.2	1297		0.825	7.25	4150	886	173	0.15	0.17	7672	23		9.8	7.9	41	739	251	11.7
CN-4D	01-16-95	FBD	1.07	1222		0.839	7.05	3917	800	138	0.26	0.84	7031	19	4	10	9	33	742	286	11
CN3RD	09-13-91	FBD	0.35	922	19.6	0.094	8.89	400	25	7	1.39		276	382		75.1	12	6	527	489	10.6
Downhole samples (acid fluids) (collected using purged KKA sampler)																					
			Depth mVD																		
CN-1	09-04-89	SHUT	1150				3.2	1300	144	9	9.4	58.4	1713	884			49.3	14	572		
CN-1	09-0789	SHUT	1200				3.8	1260	140	6	10.2	35.4	1615	810			22.9	15	557		
CN-1	09-18-89	SHUT	1400				3.4	1150	123	17.4	8.8	38.1	1590	975				16	592		
CN-1	09-19-89	SHUT	1550				4.1	1400	285	14.2	14.4	26.2	1948	827			10.6	15	533		
CN-3D	05-08-90	SHUT	1250				5.1	2600	554	89.4	1	28	4950	96				27	677		
CN2RD	06-19-91	SHUT	1775				2.9	575	37	11.3	4.2	44.2	177	894			4.3	4	356		
CN2RD	06-20-91	SHUT	1600				2.6	515	45	10.8	6.7	67.2	142	1056			37	4	466		
CN2RD	06-29-91	SHUT	1410				4.3	370	32.6	8.7	3.6	60.2	316	673			107	7	314		

* Total composition in water phase at sampling pressure (SP); ** Total composition in steam phase at sampling pressure;
Abbreviations: WHP - well head pressure; FBD - full-bore discharge; BPP - back pressure plate or orifice plate with different diameters;
mVD - meters vertical depth; TMF - total mass flow; Hd - discharge enthalpy.

2.3 Blockage history and mineral composition

As early as 1983, a blockage inside the wellbore of CN-1 was detected. The initial blockage, consisting of 90% corrosion products and 10% anhydrite, was found in this well at 1599 mVD on May 11, 1983. A subsequent survey in May 1984 located the blockage at 1593 mVD, and then it apparently extended to 1598 mVD where it was detected in September 1984. Scraper samples yielded corrosion products (40%), cuttings (30%), calcite (20%), and anhydrite (10%). In February 1990, the obstruction was detected at 1383 mVD and the composition was determined to be mainly anhydrite (46%) with significant amounts of opaques, vermiculite, cuttings, and carbonates. The well was then cleaned by a drilling rig prior to commissioning. During the production stage, wellhead pressure started to decline and a second rig cleaning was carried out. Deposition however continued to take place. During the latest survey conducted in May 1994, the blockage was detected at 1019 mVD and the composition was mostly anhydrite (76%) with corrosion products and some cement and formation rock indicating casing corrosion.

In well CN-3D, the blockage was detected at 1076 mVD in November 1994, when the well was on-line to the power plant. The deposits were composed of 90% anhydrite and 10% pyrite. In July 1995, the blockage extended up to 886 mVD and the output of the well declined significantly. Details of petrological analyses of the minerals collected from the wellbores are shown in Table 3.

TABLE 2: Cawayan production representative discharge chemistry

Well	Date	BPP	WHP	Hd	SP	pH	Concentration in mg/kg *												mmole/100moles**		
			Mpa	kJ/kg	MPa	25°C	Na	K	Ca	Mg	Fe	Cl	SO_4	H_2S	HCO_3	TCO_2	B	SiO_2	CO_2	H_2S	NH_3
CN-1	09-24-93	FBD	1.2	1216	0.094	7.86	4581	897	226	0.25	0.39	8519	26		3.1	0.88	374	830	207	7.1	2
CN-1	11-09-93	FBD	0.96	1216	0.769	7.13	4140	722	196	0.21	0.27	7780	29		12.2	7.92	322	698	230	4.8	1.69
CN-1	01-03-94	FBD	0.94	1193	0.784	7.01	3981	629	186	0.29	0.27	6994	46		7.32	12.3	301	714	232	13.40	
CN-1	03-19-94	FBD	0.93	1214	0.728	6.82	3667	717	199	0.42	0.27	6649	55	0.68	12.8	11.5	284	701	257	6.9	
CN-1	04-03-94	FBD	0.94	1214	0.784	7.04	3453	621	196	0.38	0.39	6402	53	0.35	150		260	667	255	7.7	
CN-1	05-30-94	FBD	0.98	1122	0.797	6.35	3779	647	167	0.34	1.04	6854	50.1		9	6	280	690	200	11.20	
CN-1	06-29-94	FBD	0.91	1122	0.784	6.55	3509	654	171	0.47	0.29	6496	61		10	9	260	681	250	11	
CN-1	07-27-94	FBD	0.91	1212	0.772	6.73	3496	592	186	0.63		6175	60		12	10	250	640	288	14	
CN-1	08-29-94	FBD	0.81	1212	0.756	6.48	4485	563	170	0.72		5986	68		9	10	260	627	326	8.3	
CN-1	09-26-94	FBD	0.77	1322	0.728	6.55	3120	564	157	0.81	1.08	6099	60		8	6	240	616	312	8.6	
CN-1	10-28-94	FBD	0.8	1207	0.777	6.57	3424	561	159	0.66	0.17	5962	49		12	12	430	637	326	7.1	
CN-3D	12-13-93	FBD	1.06	1253	0.811	7.2	4431	879	182	0.13	0.4	7693	21		19.5	31.7	39	731	239	12.15	4.59
CN-3D	03-24-94	FBD	1.05	1227	0.834	7.32	4220	837	194	0.28	0.5	7597	34		14	12	39	722	188	9.20	
CN-3D	04-21-94	FBD	0.95	1232	0.832	7.1	4100	861	178	0.31	0.32	7626	35.8			7	38	730	173	7.00	
CN-3D	05-18-94	FBD	0.98	1232	0.839	6.95	4185	854	152	0.4	0.24	7542	42		15	11	38	726	205	12.2	2.89
CN-3D	06-17-94	FBD	0.94	1232	0.811	7	3941	848	158	0.57	0.35	7394	52		11	9	57	706	188	9.60	
CN-3D	07-21-94	FBD	0.96	1232	0.811	7.08	4017	819	158	0.83	0.2	7199	48		17	16	37	716	262	18.8	
CN-3D	08-17-94	FBD	0.92	1232	0.825	6.99	3655	832	150	0.93		7077	51		13	12	36	716	244	16.4	
CN-3D	09-20-94	FBD	0.84	1232	0.749	7.2	3783	786	137	1.29		6912	59		6	6	34	699	369	37.7	3.68
CN-3D	10-20-94	FBD	0.9	1190	0.804	6.93	3733	724	126	1.54		6483	54		16	12	33	684	247	9.40	
CN-3D	11-16-94	FBD	0.92	1222	0.804	7.03	3422	762	122	1.59		6581	58		9	7	26	777	204	12.3	
CN-3D	11-22-94	FBD	0.94	1222	0.811	6.88	3369	762	136	1.65		6803	56		10	7	34	727	211	9.80	
CN-3D	12-02-94	FBD	0.83	1222	0.804	7.16	3454	709	127	1.65		6348	62		7	2	32	665	214	11.6	
CN-3D	12-16-94	FBD	0.91	1222	0.784	6.86	3872	753	138	1.94		6739	60		16	3	33	711	215	8.70	
CN-3D	12-29-94	FBD	0.87	1222	0.804	6.57	3708	728	124	-		6544	62		-	-	33	689	208	9.00	
CN-3D	01-04-95	FBD	0.89	1251	0.804	6.94	3547	726	128	2.25		6411	66		6	6	32	602	204	9.00	
CN-3D	01-11-95	FBD	0.908	1251	0.811	6.76	3498	734	120	2.34		6284	61		8.5	8	31	681	240	9.00	
CN-4D	02-13-95	FBD	1.14	1216	0.874	6.96	3603	762	131	0.17		6996	20		14	13	32	738	143	8.00	

* Total composition in water phase at sampling pressure (SP)

** Total composition in steam phase at sampling pressure

3. DESCRIPTION OF PRESENT WORK

This study is essentially a detailed analytical evaluation of chemical data from wells in which anhydrite deposition has taken place, utilizing speciation and reaction path programmes. Saturation conditions of the fluids with respect to anhydrite are determined using the speciation programmes WATCH 2.1 (Arnórsson et al., 1982; Bjarnason, 1994) and SOLVEQ (Spycher and Reed, 1990). Simulation runs, varying parameters such as pH and temperature, are conducted to determine how the fluid chemistry will change especially with respect to anhydrite saturation. The reaction path programme CHILLER (Spycher and Reed, 1992) is used to simulate fluid-fluid mixing of a neutral geothermal brine and a high-sulphate acid downhole fluid, simulate the effect of sodium chloride addition on anhydrite deposition, and evaluate the effect of $CaCl_2$ injection in the acid zones. The changes with time of the concentration of several chemical parameters are evaluated as indicators of deposition. The variation in several calcium and sulphate species resulting from simulation runs are closely examined in order to establish their behaviour and their effects on anhydrite saturation at different conditions. The CHILLER programme is also used to simulate the effects of NaCl, Na_2HPO_4, and HCl as possible inhibitors of anhydrite deposition.

TABLE 3: Mineral composition of wellbore deposits

Depth	Date	Composition	%
Well CN-1			
1599 mVD[a]	May 11, 1983	Corrosion products	90
		Anhydrite	10
1593 mVD[a]	May 28, 1984	Cuttings	60
		Corrosion products	30
		Anhydrite	10
1598 mVD[a]	Sept. 19, 1984	Corrosion products	40
		Cuttings	30
		Calcite	20
		Anhydrite	10
1383 mVD[b]	Feb. 21, 1990	Anhydrite	46
		Opaques consisting of:	25
		Pyrite - 50%	
		Pyrrhotite - 40%	
		Hematite - 3%	
		Magnetite - 2%	
		Chalcopyrite - 2%	
		Goethite - 2%	
		Sphalerite - <1%	
		Bornite - <1%	
		Ilminite - <1%	
		Gold - <1%	
		Vermiculite	15
		Cuttings (Dsp, I + Qtz)	12
		Carbonates (Dol > ank > Ct)	2
1019 mVD	May 24, 1994	Anhydrite	79
		Pyrite/hematite/magnetite/goethite	15
		Cement	3
		Formation rock	3
Well CN-3D			
1076 mMD[c]	Nov. 11, 1994	Anhydrite	90
		Pyrite	10
886 mMD	July 17, 1995	-- no scraper sample --	--

[a] Petroanalysis by A.G. Reyes and E.L. Bueza, 1983-84;
[b] Petroanalysis by A.G. Reyes, 1990;
[c] Petroanalysis by S.G. Ramos, 1994.

4. REVIEW

4.1 Literature review

A great deal of experimental work on the solubility of anhydrite has been described, the most notable being that of Dickson et al. (1963); Blount and Dickson (1969); and Yeatts and Marshall (1969). Dickson et al. (1963) determined the rapid decrease of anhydrite solubility in pure water with increasing temperature at constant pressure. Blount and Dickson (1969), studied the decrease in anhydrite solubility

of variably concentrated of NaCl-H_2O solutions with temperature, at constant and variable pressures. It can be concluded on the basis of their experimental results that the solubility of anhydrite is generally controlled by temperature, pressure, and salinity. Using their experimental data from solubility studies, Dickson et al. (1963) and Blount and Dickson, (1969), deduced that in natural hydrothermal processes, anhydrite deposition can occur in the following conditions; migration of saturated solutions at constant temperature from rocks interstices governed by lithostatic pressure to fissures controlled by hydrostatic pressures; descent of saturated groundwater to hotter regions; and deposition in the pores of sedimentary rocks as a result of increase in temperature accompanying burial of accumulating sediments, from interstitial waters containing $CaSO_4$, originally entrapped during sedimentation. Direct precipitation from sea water is also a possibility as in the Svartsengi wells in Iceland where there is geochemical evidence of seawater intrusion and anhydrite deposition along structures (Jón Örn Bjarnason, pers. comm.). In the oil fields, the occurrence of calcium sulphate scale, mostly gypsum, in equipment and formation has been reported by Vetter and Phillips (1970). Several other studies of anhydrite solubility are discussed and summarized in KRTA (1983). Most of the work done in that report is based on experimental conditions different from a geothermal chemical matrix.

In geothermal utilization, the occurrence of significant anhydrite deposits in wellbores has not been much reported, possibly because of the rarity of such cases. Its impact on geothermal development cannot, however, be underestimated as can be seen from the case of the Cawayan wells.

Several formulas for calculating the solubility and equilibrium constants of anhydrite have been derived by various authors. Some are based on experimental results (e.g. Blount and Dickson, 1969) while others are derived from thermodynamic data. A selection of equations that may be applicable to geothermal fluid is presented in Appendix I.

4.2 Saturation calculation

The dissolution-precipitation reaction of anhydrite can be expressed as

$$CaSO_{4(s)} \rightleftharpoons Ca^{2+}_{(aq)} \quad SO^{2-}_{4\,(aq)} \tag{1}$$

and the reaction quotient is defined by

$$Q = (a_{Ca^{2+}} * a_{SO4^{2-}}) \, / a_{CaSO4} \tag{2}$$

where a is activity which is unity for pure solid minerals like anhydrite.

As with any chemical reaction, this either absorbs or releases energy, the Gibbs free energy of reaction, expressed as

$$\Delta Gr = \Delta Gr^\circ + RT \ln Q \tag{3}$$

where R is the gas constant, T is absolute temperature (K), and ΔGr° is the standard Gibbs free energy usually presented in the literature for 25°C and 1 bar.

ΔGr° can be calculated at different temperatures from available thermodynamic data on C_p (heat capacity), ΔHr° (heat of reaction), and S° (entropy), using established thermodynamic relationships. ΔGr° is defined as

$$\Delta Gr^\circ = RT \ln K \quad (4)$$

where K is the thermodynamic equilibrium constant.

At or near equilibrium conditions (i.e. no flow of energy is taking place), $\Delta Gr = 0$, thus Equation 3 becomes

$$\Delta Gr^\circ = -RT \ln Q \quad (5)$$

and substituting Equation 4 into this yields

$$RT \ln K = -RT \ln Q \quad (6)$$

Q can be calculated from results of laboratory analysis for calcium and sulphate speciated at desired temperature, using Equation 2, while K is calculated from ΔGr° using Equation 3. So, basically the determination of saturation conditions is a comparison between log K and log Q values. When log Q exceeds log K (that defines the amount of Ca^{2+} and SO_4^{2-} ions a solution can hold at a given temperature in a thermodynamic equilibrium system), supersaturation occurs and deposition may take place. Anhydrite saturation is thus governed by the activity of sulphate and calcium, but the activity of these ions is affected by several factors such as pH, temperature, chemical matrix of the solution, and pressure.

5. DEPOSITION PARAMETERS

5.1 Evaluation of different formulas

Speciation programmes such as WATCH and SOLVEQ can perform iterations to solve mass-balance and chemical equilibrium equations, and compute activities, speciation, log K´s and mineral saturation at different temperatures. However, their application is not always straightforward due to some limitations to equilibrium computations (Nordstrom and Munoz, 1986). Validation by petrological analysis is helpful especially in cases where deposition samples can be obtained such as in the Cawayan wells. And thus in future applications they can be used in monitoring with more certainty.

Several equations for computing anhydrite solubility are evaluated for comparison. Four equations yielded results that are comparable. Figure 2 shows the equilibrium curves obtained from the

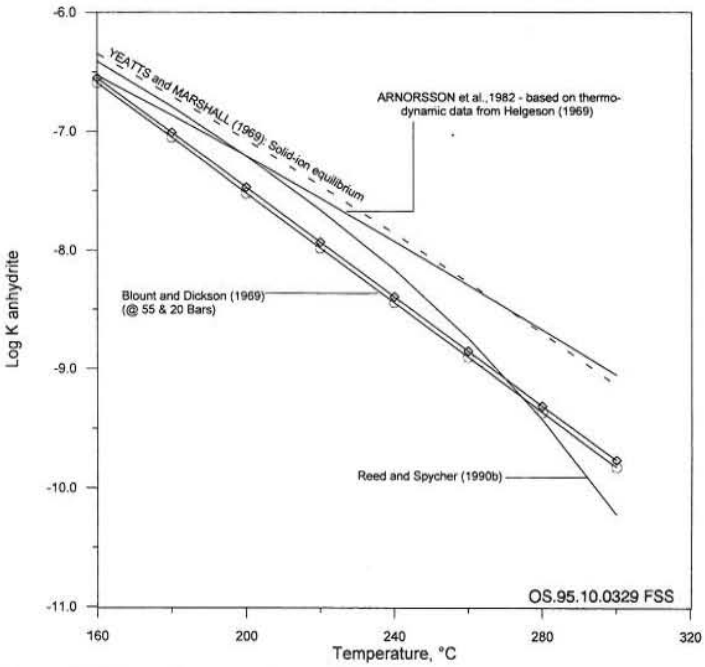

FIGURE 2: Comparison of equilibrium curves based on several formulas for calculating anhydrite solubility derived by various authors

different equations. The calculations by Arnórsson, et al. (1982), and Spycher and Reed (1990) are incorporated in the speciation programmes used in this study. Computations of their log K values for anhydrite are mostly based on thermodynamic data from Helgeson (1969). Significant deviations of the two curves from each other are observed above 200°C, possibly because of the unreliability of some thermodynamic data above this temperature (Arnórsson, et al., 1982), resulting in discrepancy in the calculated log K values. The two equations are validated using well samples collected during anhydrite deposition. Both equations show supersaturation conditions during the deposition process with results from WATCH yielding a higher degree of supersaturation.

Blount and Dickson's (1969) equation is based on experimental data from H_2O and H_2O-NaCl solutions, and pressure effect is incorporated. This equation yielded relatively low values of log K at low temperatures, but at high temperatures the results were similar to those of Reed and Spycher (1990). Yeatts and Marshall's (1969) equation is based on solid-ion equilibrium and the calculated equilibrium curve is almost identical to that of Arnórsson, et al. (1982).

The different log K values calculated using the various equations are given in Table 4. The values are significantly different especially at temperatures above 200°C. But in application, they yielded similar saturation conditions.

TABLE 4: Comparison of different log K values for anhydrites

Temp.	Blount and Dickson, 1969			Arnórsson	Yeats and	Reed and
(°C)	5 bars	55 bars	20 bars	et al., 1982	Marshall, 1969	Spycher, 1990
160	-6.613	-6.550	-6.590	-6.529	-6.345	-6.410
180	-7.075	-7.010	-7.050	-6.863	-6.701	-6.790
200	-7.538	-7.470	-7.520	-7.207	-7.072	-7.210
220	-8.000	-7.930	-7.980	-7.561	-7.457	-7.660
240	-8.463	-8.390	-8.440	-7.923	-7.856	-8.160
260	-8.925	-8.850	-8.850	-8.292	-8.270	-8.740
280	-9.388	-9.310	-9.310	-8.667	-8.697	-9.420
300	-9.850	-9.760	-9.760	-9.048	-9.138	-10.220

5.2 Saturation conditions and mineral-solution equilibria

The saturation conditions of the Cawayan fluids with respect to anhydrite during baseline and production stages are determined using both the WATCH and the SOLVEQ programmes. Results in Figure 3 show that fluids from production wells (CN-1/CN-3D/CN-4D) are initially saturated (or slightly undersaturated) with anhydrite, suggesting near equilibrium with this mineral. During the production stage, data points from the producing wells CN-1 and CN-3D plotted above the anhydrite equilibrium curve suggesting that the fluids have become supersaturated with respect to anhydrite. Correspondingly, some geochemical parameters started to exhibit specific trends with time, and months later, the wellhead pressures started to decline. These results show that both speciation programmes are sensitive to anhydrite saturation changes and can be effectively used for monitoring critical wells.

The acid and dilute fluids in the reinjection wells CN-2RD and CN-3RD, and the downhole samples from CN-1 and CN-3D are all supersaturated with respect to anhydrite (Figure 3). Evaluation of fluid equilibria from SOLVEQ runs, with some minerals identified from petrological analysis showed apparent equilibrium only with quartz (Figure 4). The curves did not exhibit any common point of intersection

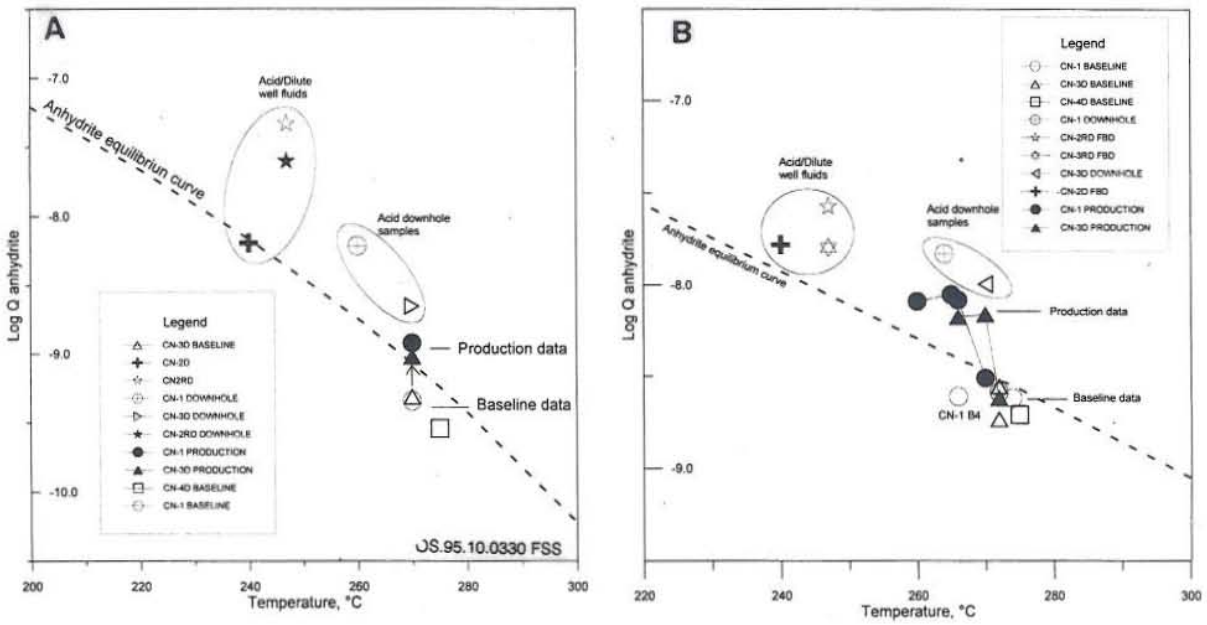

FIGURE 3: Anhydrite saturation of Cawayan well fluids (baseline and production data);
a) using the SOLVEQ programme by Spycher and Reed (1990);
b) using the WATCH programme by Arnórsson et al. (1982)

along the log (Q/K)=0 line indicating that these fluids have not attained equilibrium with the identified minerals except quartz. The acid well fluids are also supersaturated with iron minerals such as pyrite, and hematite because of elevated concentrations of iron, probably derived from dissolution of casing. The fluid in CN-3RD which is slightly alkaline despite its high sulphate concentration and proximity to the acid fluid wells, is also supersaturated with respect to carbonate minerals such as dolomite, $CaMg(CO_3)_2$, and calcite suggesting the occurrence of high CO_2 concentrations in the well fluid. For anhydrite, all well fluids, except CN-2D, plotted above the equilibrium line suggesting that this mineral is in excess in the solutions. The presence of sulphate-bearing minerals such as anhydrite and alunite, $KAl_3(OH)_6(SO_4)_2$, in the formation rocks of the wells is an indication of possible precipitation of anhydrite from the fluid, and interaction with the rocks. However, further investigation of fluid equilibria with other key and associated minerals found in the wells is necessary before this can be established.

The high-sulphate acid fluids in Bacman have been interpreted to have originated from the oxidation of H_2S in the vadose zone, and subsequently percolated to deeper levels (Solis et al., 1994). The results of sulphur and oxygen isotope analyses support this postulate. These fluids are believed to be the main source of excessive amounts of sulphate and the major cause of anhydrite deposition in the Cawayan wells.

5.3 Speciation

Another set of data obtained from WATCH and SOLVEQ is on the various calcium and sulphate species (Figure 5) which may be directly or indirectly involved in the deposition process. Evaluation of these species during supersaturation conditions of well fluids from CN-1 and CN-3D showed that at 270°C, about 64% exist as $CaCl^+$, 23% as $CaCl_2$, 5% as $NaSO_4^-$, 3% as KSO_4^-, 3% as Ca^{2+}, and 1% as SO_4^{2-}. According to the results of WATCH in which the $CaCl^+$ and $CaCl_2$ species are not incorporated, the major ion is Ca^{2+} at 57% while SO_4^{2-} accounts for only 2%. The results of the SOLVEQ run show

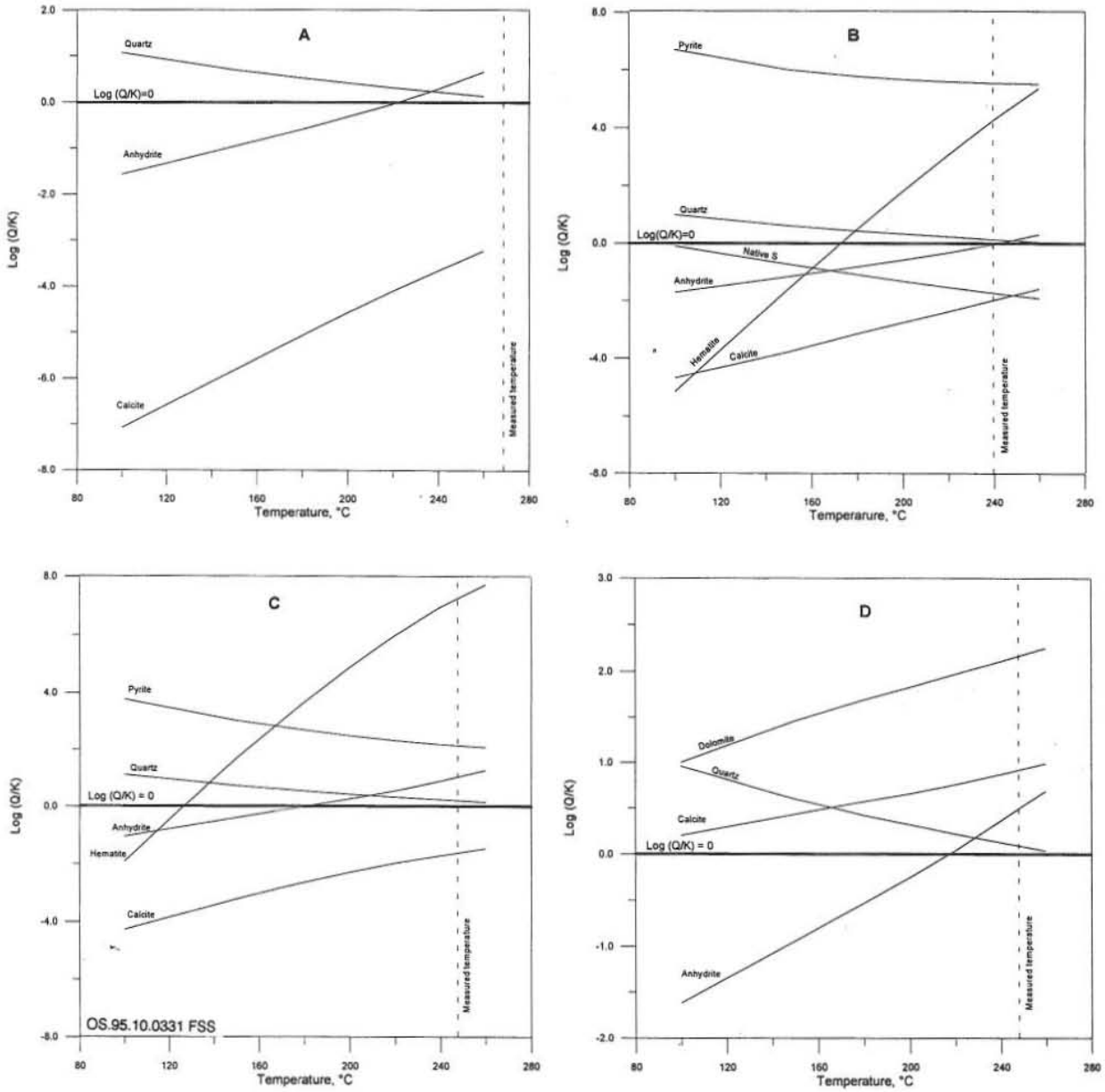

FIGURE 4: Mineral-solution equilibria of Cawayan high-sulphate and acid fluids with selected minerals identified from petrological analysis; a) CN-1 downhole sample; b)CN-2D fluid; c) CN-2RD fluid; d) CN-3RD fluid

that the calcium ions prefer association with chloride ions, while sulphate is more associated with sodium and potassium ions. The "free" calcium and sulphate ions that are directly involved in anhydrite deposition account for very small percentages of the total species. These amounts are however sufficient to cause significant deposition. Sample calculations for CN-3D data show that an increase of a mere 1.02×10^{-6} in molal activity (~1 mg/kg increase in reservoir sulphate concentration) can lead to supersaturation. This shows that for initially saturated fluids, a very slight increase in sulphate or calcium activity can cause supersaturation and possibly deposition. Temperature also has significant effects on the activity of calcium and sulphate species. This is discussed in Chapter 7.3.

For the downhole high-sulphate acid fluid, speciation results show a different distribution at 270°C. The dominant species are $NaSO_4^-$ (44.9%), SO_4^{2-} (16.4%), HSO_4^- (16.1%), and KSO_4^- (11.0%). Other sulphate

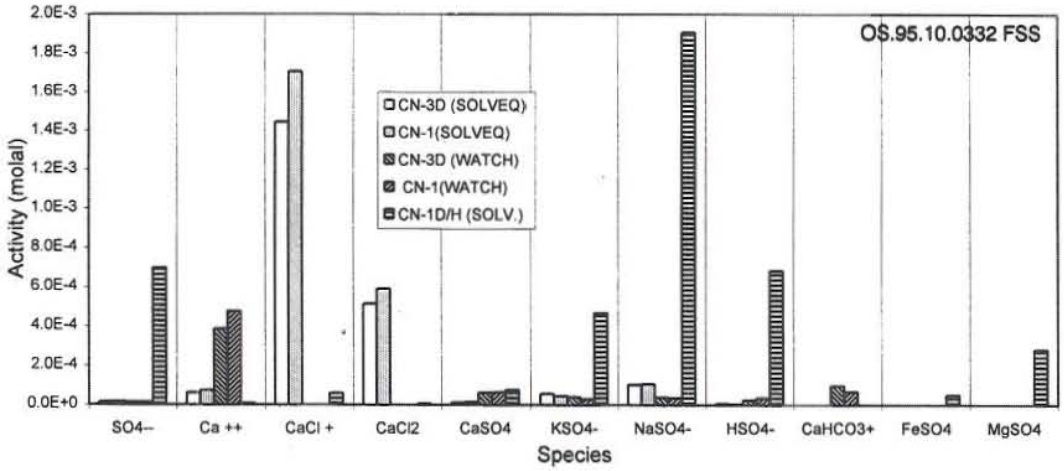

FIGURE 5: Calcium and sulphate species distribution of CN-1 and CN-3D supersaturated fluids, and CN-1 high-sulphate acid downhole water at 270°C

forms, practically absent from the production brine, such as $FeSO_4$ and $MgSO_4$ are also present because of the relatively high concentrations of iron and magnesium. These results reveal the source of high sulphate ion activity responsible for the anhydrite deposition. However, despite the very high sulphate concentration, its activity does not make it the dominant species. This implies that if sulphate association with sodium, potassium, magnesium, iron, and hydronium ions can be increased, the tendency for the fluid to deposit anhydrite can be reduced.

5.4 Geochemical indicators of anhydrite deposition

Evaluation of the chemistry of the Cawayan fluids before and during anhydrite deposition yielded chemical parameters that exhibited specific trends with time and may thus be useful as indicators. These parameters are sulphate, calcium, magnesium, chloride, and silica. A decrease in pH was also detected, but it is not very pronounced and fairly erratic. These chemical parameters already exhibit unusual trends long before physical changes in the wells such as wellhead pressure (Figure 6) and output decline become measurable. Data used in the plots covered a period of about fifteen months from baseline to production stages.

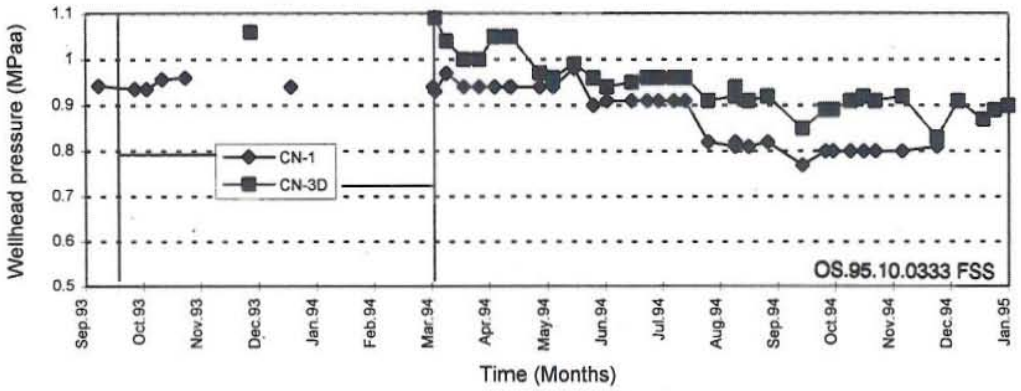

FIGURE 6: Wellhead pressure with time during anhydrite deposition, vertical lines indicate the start of anhydrite supersaturation in CN-1 and CN-3D fluids

Sulphate

Figure 7 shows the sulphate concentration trend with time. The sulphate concentration is increased during deposition from 23 mg/kg (baseline saturation concentr.) to 71 mg/kg for CN-1, and from 21 mg/kg to 66 mg/kg for CN-3D. The increase in sulphate indicates the inflow of the mixing fluid identified at the upper horizon of the wells during downhole sampling. These fluids have earlier been characterized to be acid and contain high sulphate, ranging from 810-975 mg/kg for CN-1 and 62-96 mg/kg for CN-3D. Sulphate appears to be a sensitive indicator of anhydrite deposition, increasing abruptly as supersaturation occurs and then exhibiting a steady increase throughout the deposition process suggesting a continuous influx of the mixing fluid.

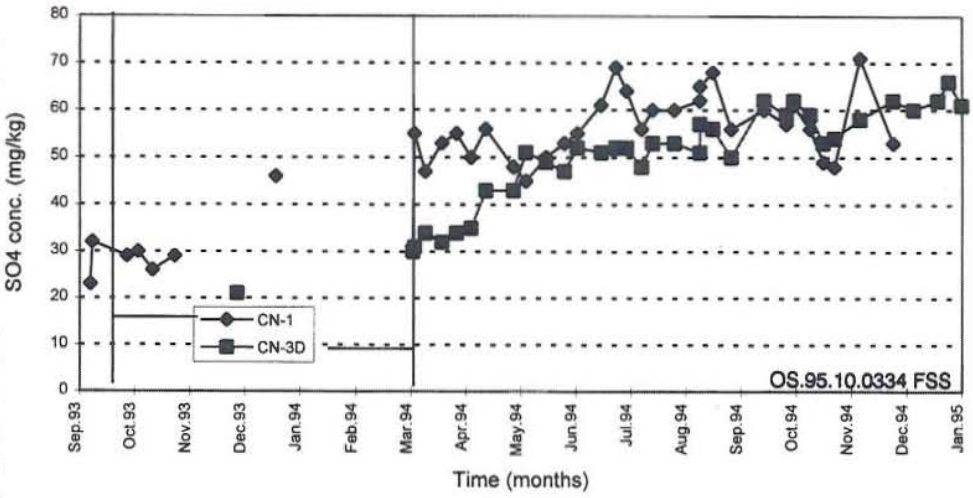

FIGURE 7: Sulphate concentration with time during anhydrite deposition, vertical lines show start of anhydrite supersaturation for CN-1 and CN-3D fluids

Calcium

Calcium concentration increased during the early stages of supersaturation (Figure 8), then decreased abruptly and maintained a steady decline as deposition proceeded. Calcium concentration at the wellhead decreased gradually from about 196 mg/kg to 146 mg/kg in CN-1, and 180 mg/kg to 120 mg/kg in CN-3D. Since the mixing fluid is depleted in calcium, the calcium from the production brine is continuously being consumed by the excess sulphate during the formation of anhydrite.

Significant fluctuations are also observed especially for CN-1 indicating possible fluctuations in the rate or the amount being deposited. The decreasing trend however, is an indication that the rate of deposition is increasing, probably because of the increasing acid-sulphate fluid influx.

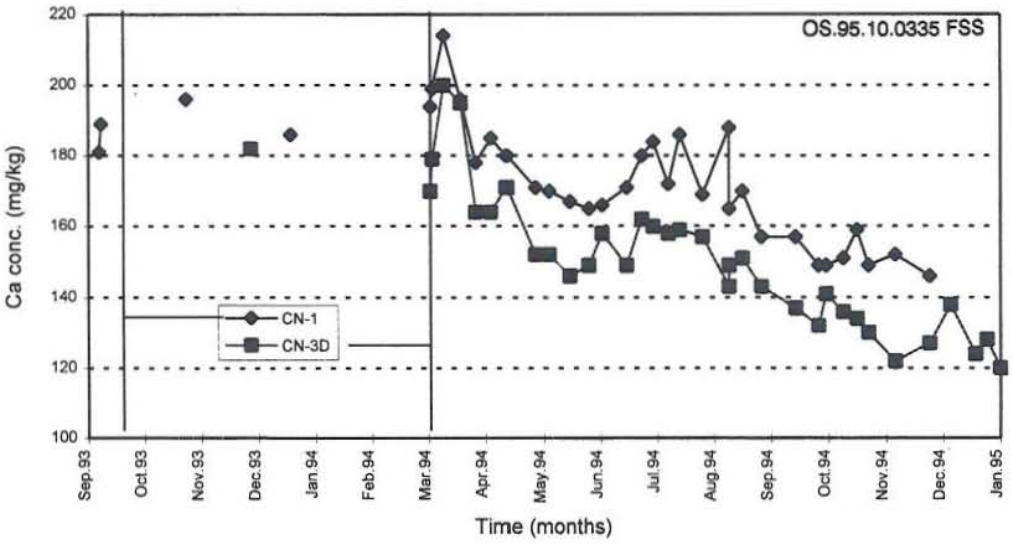

FIGURE 8: Calcium concentration with time during anhydrite deposition, vertical lines indicate start of anhydrite supersaturation for CN-1 and CN-3D fluids

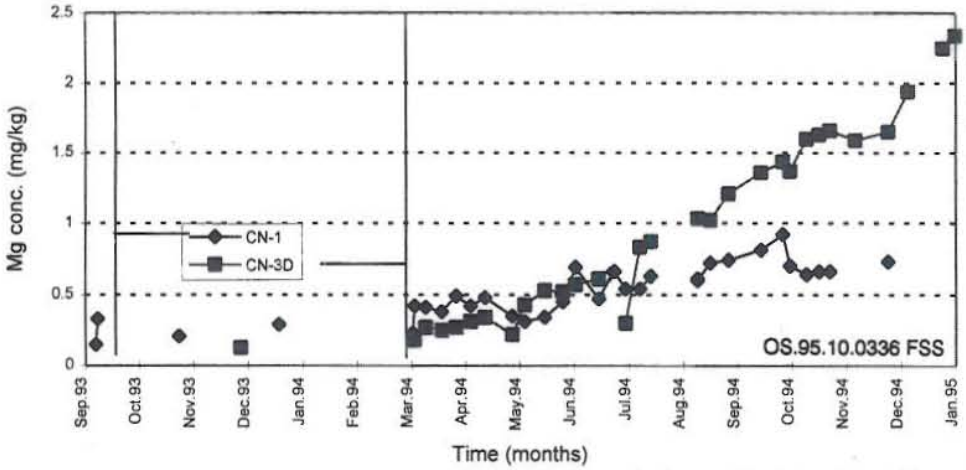

FIGURE 9: Magnesium concentration with time during anhydrite deposition, vertical lines indicate start of anhydrite supersaturation for CN-1 and CN-3D

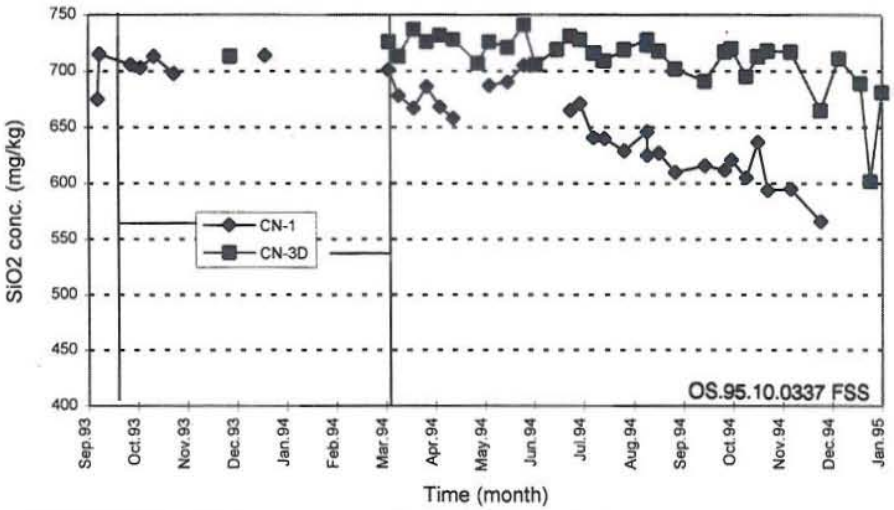

FIGURE 10: Silica concentration with time during anhydrite deposition, vertical lines indicate start of anhydrite supersaturation in CN-1 and CN-3D

Magnesium, chloride, and silica

Figures 9, 10, and 11 show the magnesium, chloride, and silica concentration trends with time. Although not directly involved in anhydrite deposition, in Cawayan wells, these chemical parameters are indicators of the relatively cold and dilute acid fluids that mix with the brine. It can be seen that concentration of magnesium is increasing (Figure 9), especially during the later part of the deposition, which suggests the presence of a colder fluid. The Silica concentration (Figure 10), on the other hand, decreased especially in CN-1 indicating that the well is cooling down because of the influx of the colder mixing fluid.

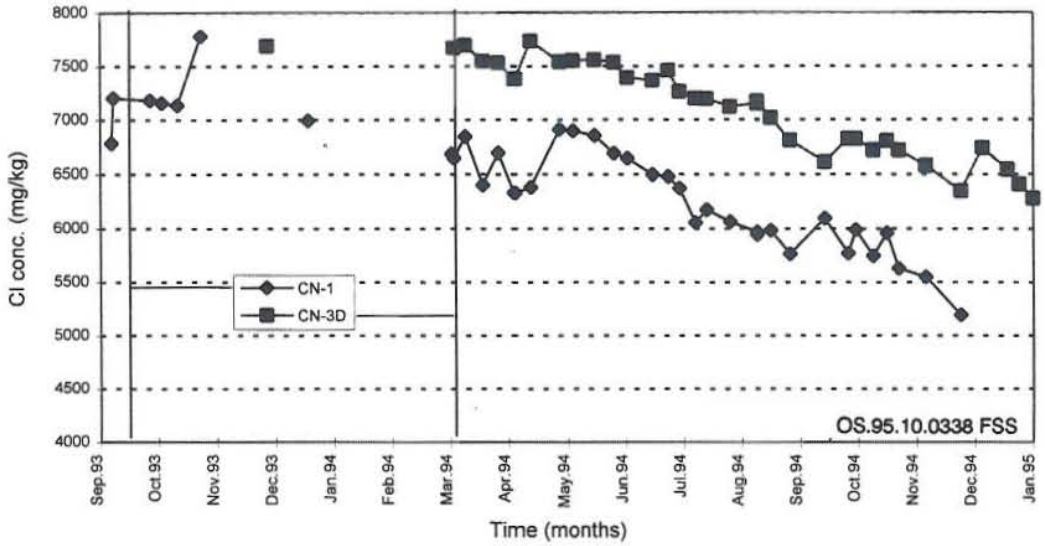

FIGURE 11: Chloride concentration with time during anhydrite deposition, vertical lines indicate start of anhydrite supersaturation in CN-1 and CN-3D

Silica concentration, however, did not respond immediately and began to decrease only during the later stages of the deposition process. In CN-3D, the drop in silica concentration is not as pronounced, possibly because of a smaller amount of mixing fluid. The chloride concentration (Figure 11) is similarly decreasing, and also shows the influx of the dilute fluid.

All these geochemical indicators continued to exhibit trends, either increasing or decreasing, throughout the deposition process with no indications of levelling-off or attainment of constant values. These results suggest that the influx of mixing fluids into the wells increases continuously and the rate of deposition is also increasing.

6. MIXING SIMULATIONS

The anhydrite deposits in the Cawayan wells have been deduced to be the end-product of mixing of high-sulphate acid fluids and calcium-rich geothermal brine. The baseline and production anhydrite saturation conditions, downhole chemistry, and trends exhibited by the geochemical indicators support this conclusion.

Reaction path programmes can provide information about the resultant mineral composition and aqueous-speciation for a given set of initial conditions and a given set of hypothetical reactions (Nordstrom and Munoz, 1986). The CHILLER programme (Spycher and Reed, 1992) is a reaction path programme that can simulate the addition or mixing of aqueous solutions, solids, or gases to an existing solution at different temperatures and mixing fractions. Most minerals and equilibrium reactions of species found in typical geothermal fluids are incorporated in this programme through its database SOLTHERM (Reed and Spycher, 1990). The "coolbrew" option of the programme is used to simulate fluid-fluid mixing of the Cawayan production fluid and the high-sulphate acid downhole water from CN-1 and CN-3D, at different temperatures. Application in this particular case is facilitated by the petrological analysis results for the deposits inside the wellbores; minerals not found are "suppressed", avoiding unnecessary equilibrations and thus computing time is faster and simulations more accurate. Mineral suppression is commonly used to disallow kinetically disfavoured minerals, selected on the judgement of the user (Spycher and Reed, 1992). Minerals suppressed in this run and the succeeding runs include quartz, chalcedony, talc, tremolite, and diopside. These minerals have been calculated by CHILLER as supersaturated, but were not detected by petrological analysis at any given time. Therefore, the suppression of these minerals has a sound basis. Samples of input data and output of the CHILLER programme are shown in Appendix II.

Figure 12 shows the results of mixing simulations. Mixing is carried out by titrating 1 kg of the baseline water sample with 0.01 to 0.10 fractions of downhole water at 270, 260, and 200°C. For CN-1, the downhole mixing fluid is collected at 1150 mVD (near the depth of deposition) with pH 3.2 and contains 884 mg/kg sulphate. Originally, the CN-1 production fluid is just saturated with anhydrite (Figure 3) with no deposition taking place. As mixing with the acid downhole fluid starts, sulphate activity begins to increase. At the 270 °C mixing temperature, deposition starts when the fraction of the downhole fluid is 0.03, with approximately 2.1×10^{-3} g of anhydrite forming. From this point, the amount of anhydrite deposited increases significantly with the amount of mixing fluid added. Calcium activity started to decrease as anhydrite formed while sulphate continued to increase because of the additional sulphate from the mixing fluid. The increase in sulphate activity is, however, not proportional to the increase in the fraction of mixing fluid added because it is to some extent consumed by anhydrite. Such behaviour of these two species is reflected in the calcium and sulphate concentrations of the wellhead samples and plotted in Figures 7 and 8 as geochemical indicators. The hydrogen ion (H^+) activity also increased slightly due to the acidity of the mixing fluid. Decrease in pH has also been measured at the surface.

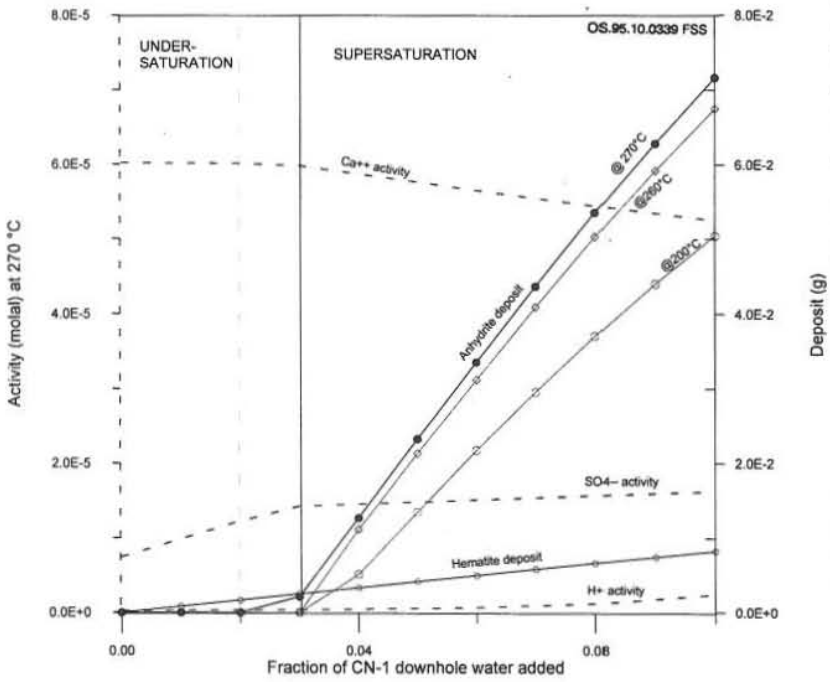

FIGURE 12: Simulated mixing of CN-1 production fluid and acidic high-sulphate downhole water at different temperatures, mixing simulation performed using the CHILLER programme; at 270°C deposition starts at mixing fraction 0.03; at 260 and 200°C deposition occurs at fraction 0.04; hematite is also deposited

Finally, for a mixing fluid fraction of 0.10 (or 10%), the amount of anhydrite deposited is estimated at 7.0×10^{-2} g. The downhole pH decreases from 6.61 to 5.62, calcium activity drops from 6.02×10^{-5} to 5.0×10^{-5} molal, and sulphate activity increased from 7.45×10^{-6} to 1.63×10^{-5} molal. Hematite deposits also formed because of the high iron content of the mixing fluid. The amount of hematite, however, is small compared with that of anhydrite. Simulations at mixing fluid temperatures of 260 and 200°C yielded similar results but smaller amount of anhydrite deposits, and deposition starts in all cases at a mixing fraction of 0.04. This simulation result from CN-1 agrees with previous evidence that mixing of the two different fluids is the cause of anhydrite deposition, and validates the thermodynamic conditions in the programme for this case. The results can also be used (if properly calibrated with pertinent data such as flowrate, casing volume and the results of caliper or go-devil surveys) to estimate the volume of deposits formed and, thus, might be useful in predicting how long a well can produce before cleaning operations are scheduled.

The results of a similar simulation with CN-3D fluids did not yield supersaturation, probably because of the much lower sulphate concentration of the mixing fluid used (96 mg/kg). The deposition in CN-3D, however, indicates that a more sulphate-rich fluid is mixing with the production brine.

7. SATURATION CHANGES AT DIFFERENT CONDITIONS

7.1 Effect of pressure (varying back pressure plates)

The effect of pressure has been studied in previous experimental work. In pure water solutions, and in NaCl-H_2O solutions, the solubility of anhydrite is significantly affected by large pressure differences (about 500 bars) (Dickson et al., 1963; and Blount and Dickson, 1969). In normal geothermal production, the pressure inside the wellbore can only be varied over a very limited range through the use of back pressure plates; for example from 6 to about 20 bars for CN-1. Anhydrite solubility is not significantly affected over this pressure interval (Blount and Dickson, 1969), as shown in Figure 2 and Appendix I. In actual operations, varying pressure plates will probably affect anhydrite saturation through changes in the interplay of the various production zones of the well which involve changes in sulphate concentration and temperature between zones. In CN-1, for example, discharge fluid at BPP B4 during the baseline stage yielded the lowest concentration of sulphate, and the most pronounced

undersaturation condition with respect to anhydrite (Figure 3b). The reduction in the anhydrite solubility product is probably caused by the prevalence of a fluid from a different feed zone rather than the increase in pressure.

7.2 Effect of pH

Figure 13 shows the effect of pH changes on anhydrite solubility and on the activities of sulphate and calcium species. The SOLVEQ programme (Spycher and Reed, 1990) which has an option for changing pH is used to simulate consequences of pH increase and decrease. Lowering the pH, i.e. increasing the molar concentration of hydrogen ions revealed a significant effect on anhydrite supersaturation. Decreasing deep water pH from the original values of 6.12 and 6.39 for CN-1 and CN-3D respectively, to pH 5.0 resulted in normal saturation and eventually in undersaturation as pH is lowered continuously. The effect of lowered pH is a decrease in SO_4^{2-} activity and a corresponding increase in HSO_4^- activity. Formation of bisulphate ion is favoured at high hydrogen ion activity (low pH) as shown by the reaction

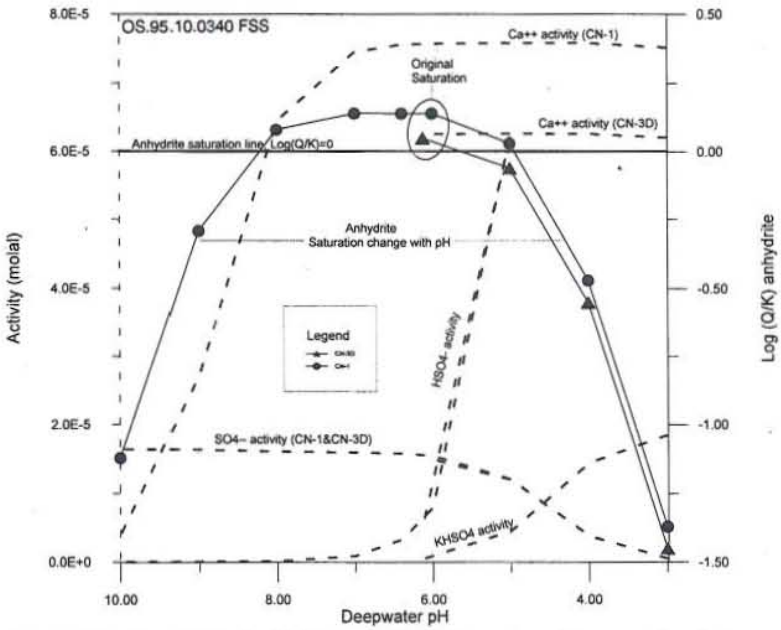

FIGURE 13: Effect of pH on anhydrite saturation, and calcium and sulphate activity at 270°C. pH changes are simulated using the SOLVEQ programme with samples from CN-1 and CN-3D supersaturated with anhydrite

$$SO_4^{2-} + H^+ \leftrightharpoons HSO_4^- \qquad (7)$$

where increase in H^+ activity will shift reaction to the right. The activity of $KHSO_4$ also increased as some bisulphate associated with potassium ions (K^+). The lower sulphate activity results in a lower anhydrite activity product as calcium activity remains constant while pH is decreased. This pH effect shows that in CN-1 and CN-3D, the pH of the mixture from which anhydrite is deposited is probably near neutral despite the low pH of the mixing fluids. At pH above 8, the anhydrite activity product will also decrease as calcium will be consumed by the formation of calcite, and other associated calcium species.

7.3 Effect of temperature

As mentioned earlier, the effect of temperature on anhydrite solubility has been studied experimentally by Dickson et al. (1963) and Blount and Dickson, (1969). Both SOLVEQ and WATCH have options for cooling and heating. Simulation runs with these programmes show that indeed as temperature decreases, the activities of calcium and sulphate ions increase, i.e. the solubility of anhydrite increases and undersaturation is approached (Figure 14). Thus at lower temperatures more anhydrite can be dissolved and the tendency to deposit is lower. This is supported by the higher thermodynamic equilibrium constants for anhydrite at lower temperatures. In CN-1, a 10°C drop in temperature will result in undersaturation.

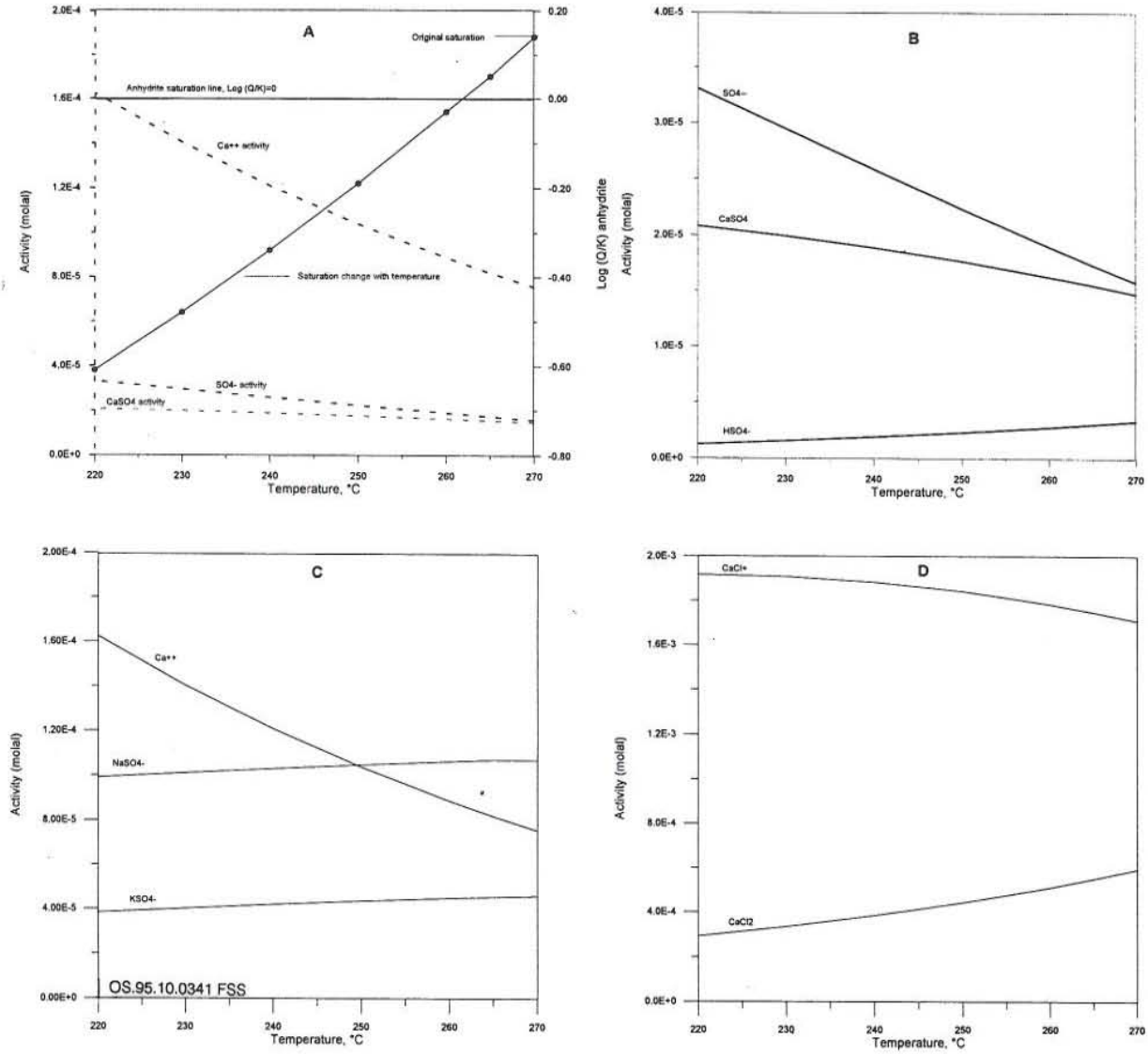

FIGURE 14: Effect of temperature on anhydrite saturation, and sulphate and calcium species activity; simulation carried out using the SOLVEQ programme with sample from CN-1 supersaturated with respect to anhydrite

Figure 14 also shows the effect of temperature on calcium and sulphate species. The activities of sulphate species such as $NaSO_4^-$, KSO_4^-, and HSO_4^- increased slightly with temperature indicating that these species become more associated with sulphate ions at higher temperature. However this increase in association is not enough to offset the decrease in solubility of sulphate at higher temperature and prevent the precipitation of anhydrite. Calcium chloride ($CaCl_2$) concentration also increased with temperature indicating more association of calcium and chloride ions. These temperature-speciation results imply that if these associations at higher temperatures of sulphate and calcium ions with Na^+, K^+, H^+, and Cl^- ions can be enhanced, the tendency for anhydrite to deposit will be reduced.

7.4 Effect of NaCl addition

The effect of NaCl on anhydrite solubility at different pressure and temperature has been investigated by Blount and Dickson, (1969). Their experimental conditions covered wide ranges of temperature and pressure and their results have shown that anhydrite is more soluble in NaCl solution than in pure H_2O.

Their experiments, however, were conducted in a NaCl-H_2O-anhydrite solution in which the chemical matrix is very different from that of a geothermal brine such as that of the Cawayan wells.

The CHILLER programme is used to simulate the effect of NaCl addition on the supersaturated fluid from well CN-1. One kg of CN-1 fluid is titrated with 0.01 to 0.10 fractions of one mole NaCl at 270°C. The result (Figure 15) shows that NaCl apparently dissolves the anhydrite deposit, and converts the fluid from a supersaturated to an undersaturated condition. Initially, the fluid is depositing approximately 0.016 g of anhydrite per kg solution. Upon addition of NaCl, the amount of deposit is reduced significantly. When a fraction of 0.04 has been added, deposition stops and the solution becomes undersaturated with respect to anhydrite.

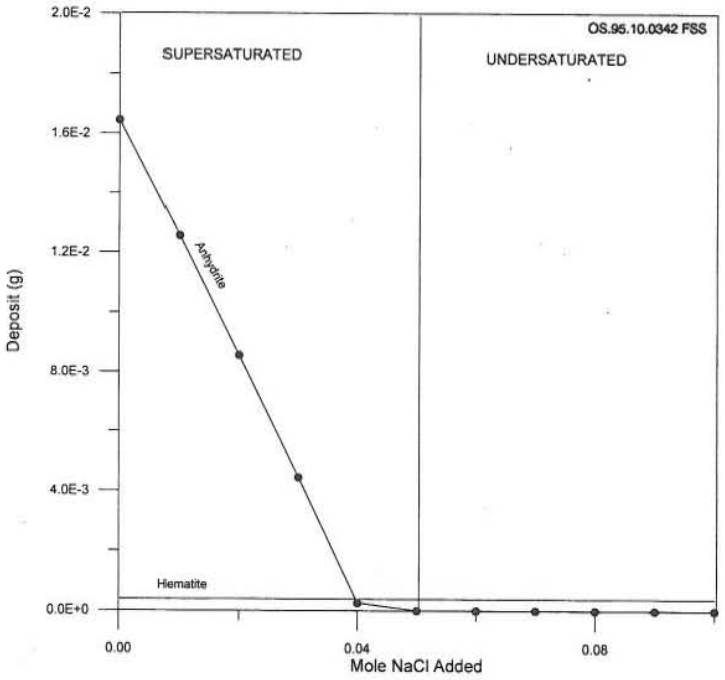

FIGURE 15: Effect of NaCl addition on anhydrite deposition; the initial deposition at the anhydrite supersaturation is ~$0.16x10^{-1}$ g/kg solution; addition of NaCl significantly reduces the amount of deposit; at 0.05 mole NaCl added, the deposition stops, and normal saturation is attained; Further addition of NaCl results in undersaturation; hematite is deposited but on a much smaller scale; simulation is carried out using CHILLER with a sample from CN-1, supersaturated with anhydrite, at 270°C

Figure 16 shows the effect of NaCl addition on the calcium and sulphate species of the supersaturated fluid. Evaluation of these species during the titration process showed that the most probable cause of undersaturation with respect to anhydrite is the significant decrease in calcium activity, and the significant increase in $NaSO_4^-$ activity. Sulphate at first, exhibited an increase in activity during titration at anhydrite supersaturation because of the apparent dissolution of anhydrite. Initially, both sulphate and calcium are present in the solid phase as anhydrite mineral; upon addition of NaCl, these ions apparently dissolve and rejoin the liquid phase. A significant amount of the redissolved sulphate associates with sodium ion to form $NaSO_4^-$. Other sulphate species such as KSO_4^- and HSO_4^- also exhibited slight increases in activity, but these associations are apparently not sufficient to consume all the redissolved sulphate. Thus some sulphate exists as free SO_4^{2-} as shown by the increase in its activity during titration at anhydrite supersaturation. Calcium ion activity exhibited a steady decline despite the dissolution because of its association with chloride as $CaCl_2$ which increased significantly, probably enough to consume all the redissolved calcium species. After normal saturation is attained, sulphate and calcium activities decline continuously with increased NaCl addition. The decrease in the activity of these two ions at constant temperature leads to a lower log Q and less tendency to deposit anhydrite. $NaSO_4^-$ and $CaCl_2$ activities continue to increase. Apparently, the effect of NaCl addition is to associate sulphate ion as $NaSO_4^-$ and calcium ion as $CaCl_2$ and thus significantly decrease the activity of unassociated calcium and sulphate ions which are responsible for anhydrite supersaturation and eventually, deposition.

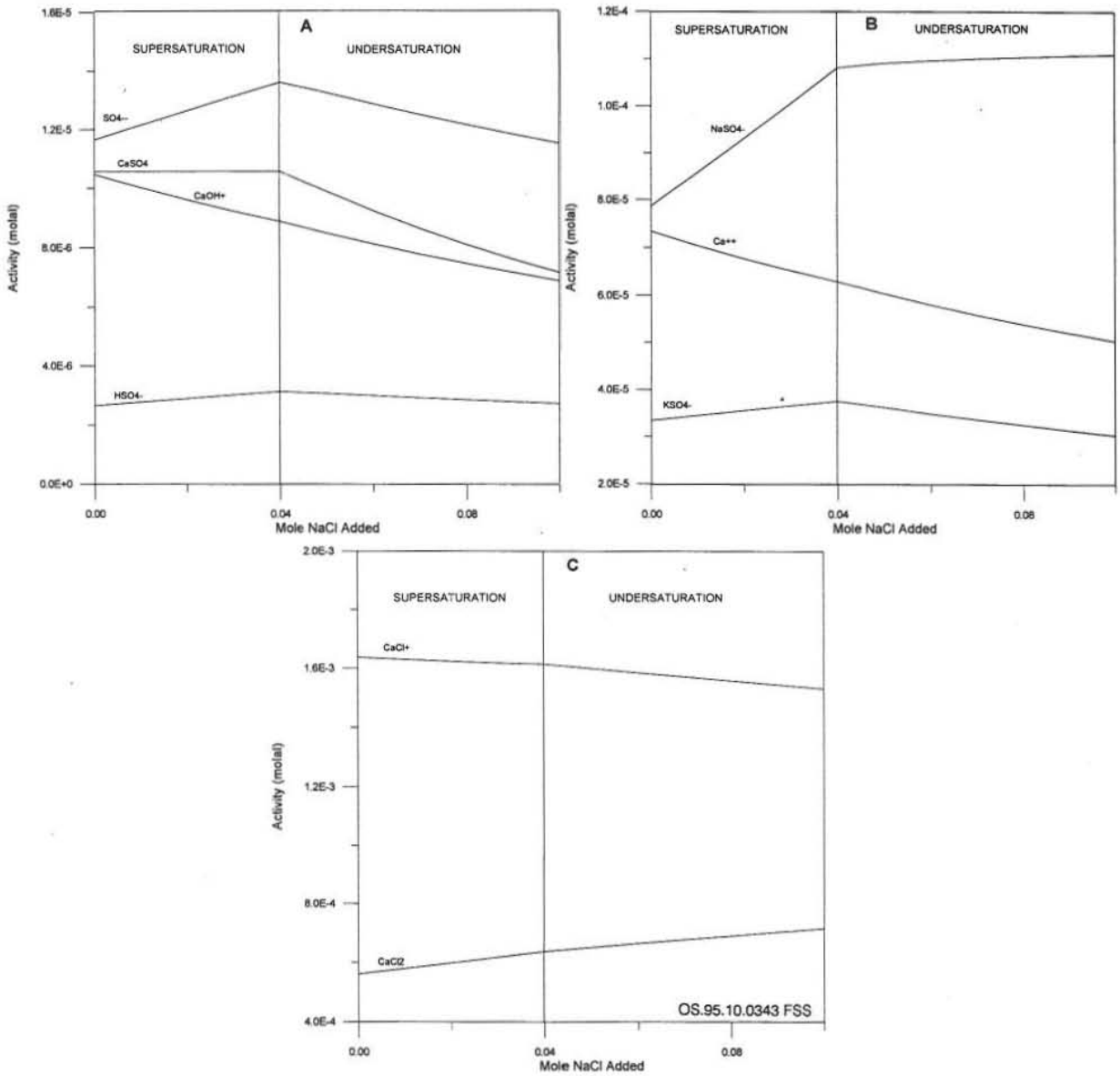

FIGURE 16: Effect of NaCl addition on calcium and sulphate species at 270°C; simulated titration using the CHILLER programme with CN-1 fluid supersaturated with anhydrite

8. INDUCED DEPOSITION - $CaCl_2$ INJECTION

The concept of inducing deposition of anhydrite in acid zones by the addition of "excess" calcium and thus forming a "barrier", sealing off acid fluids to protect the casings has been discussed in several PNOC-EDC internal reports, and has actually been practised during drilling.

The CHILLER programme fluid-fluid mixing option is utilized to simulate the mixing of high-sulphate acid fluid with $CaCl_2$ at different temperatures and mixing proportions. The purpose is to find out whether deposition is indeed induced and whether sulphate is removed from the solution.

Figures 17 and 18 show the effect of $CaCl_2$ addition on anhydrite deposition and on the activity of sulphate ions at different temperatures. The simulated mixing shows that at 235°C, immediate deposition

of anhydrite is induced at a 0.01 mole fraction of $CaCl_2$, and the sulphate activity decreased abruptly from $0.90449x10^{-3}$ to $0.51909x10^{-4}$ molal. Sulphate apparently reacts with the additional calcium ions from calcium chloride to form anhydrite.

Addition of more $CaCl_2$ resulted in a near constant rate of deposition and sulphate stabilized at an activity of about 0.3 to $0.7x10^{-5}$ molal at which normal saturation with respect to anhydrite is reached. The activity of calcium sulphate as an associated form remained constant during the titration process showing that at saturation the activity of this species does not change significantly. Titration at 150°C revealed a similar trend except that the amount of anhydrite deposit produced was smaller and the decrease in sulphate activity is more gradual and stabilized at a higher value. At 100°C, a smaller amount of deposit is formed and the sulphate activity stabilized at even higher values.

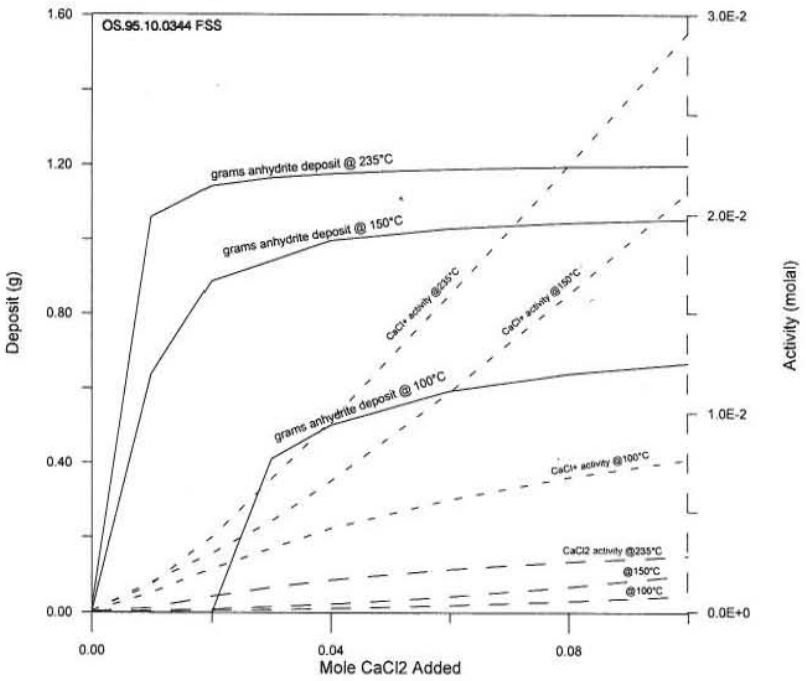

FIGURE 17: Anhydrite deposition induced by $CaCl_2$ addition at 235, 150, and 100°C; simulated mixing using the CHILLER programme with a sample from CN-1 acid high-sulphate downhole fluid

$CaCl_2$ addition also has significant effects on the various sulphate species (Figure 19). In its natural condition at the assumed temperature of 235°C, the acid-sulphate water contains bisulphate (HSO_4^-) as the major sulphate species followed by $NaSO_4^-$, SO_4^{2-}, and KSO_4^-. Other species such as $MgSO_4$, $FeSO_4$, and $KHSO_4^-$ also exist in significant amounts. Addition of $CaCl_2$ drastically reduces the activities of these species as sulphate is consumed by the induced deposition of anhydrite. The hydrogen ion activity however increases, i.e. pH decreases and the fluid becomes more acid as $CaCl_2$ is added. The dissociation of bisulphate probably controls the pH of the mixture according to Reaction 7. As more calcium is added, more sulphate is removed thus shifting the reaction to the left favouring the formation of

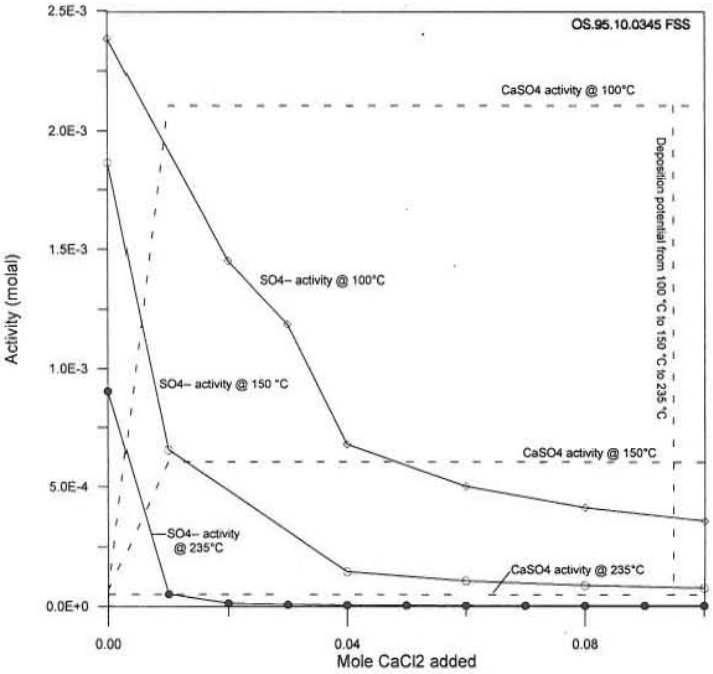

FIGURE 18: Effect of $CaCl_2$ addition on $CaSO_4$ and sulphate ion activities of high-sulphate acid downhole water from CN-1 at different temperatures; simulated mixing carried out using the CHILLER programme

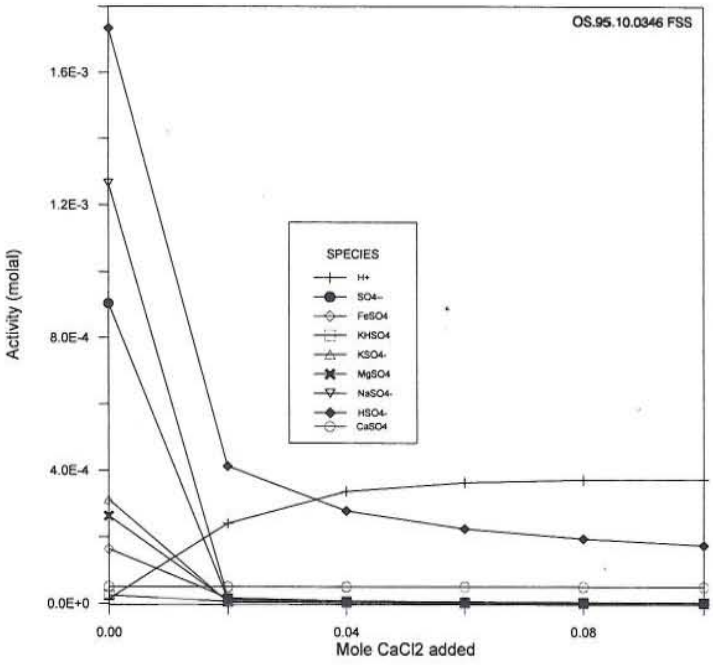

FIGURE 19: Effect of $CaCl_2$ addition at 235°C on calcium and sulphate species, and hydrogen ion activity of CN-1 high-sulphate acid downhole water

more hydrogen ions. Such a reaction may have adverse effects since the fluid becomes more corrosive as the pH decreases. The simulated mixing showed that downhole pH declines from 4.86 to 3.42 as the fraction of $CaCl_2$ added is increased from 0.01 to 0.02 (Figure 19).

These results show that injection of $CaCl_2$ at a relatively low temperature will not totally eliminate the potential of the fluid to deposit anhydrite, and that temperature plays a very critical role in this injection scheme. Since the $CaCl_2$ injectate is usually pumped at a low temperature, the temperature of the injection zone must be high enough and the heat recovery fast for the injection to be effective. Otherwise the addition of $CaCl_2$ will only increase the potential of the fluid to deposit anhydrite, especially when it comes into contact with a hotter fluid. Deposited anhydrite in the formation rocks also has the tendency to be dissolved at colder temperatures, and be redeposited at higher temperatures. Calcium chloride injection also tends to lower the downhole pH. This method, although it can probably induce "beneficial" deposition, apparently has some harmful consequences and therefore needs further evaluation in future applications.

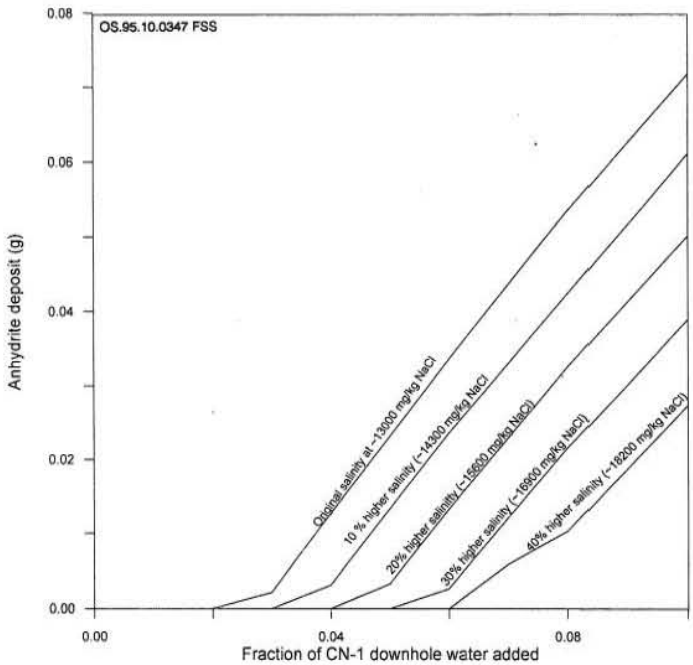

FIGURE 20: Effect of increasing salinity (NaCl conc.) on anhydrite deposition from CN-1 production fluid for 270°C and different fractions of high-sulphate downhole fluid

9. POSSIBLE METHODS OF CONTROL

9.1 $NaCl/Na_2HPO_4$ addition

Both experimental studies and simulation runs have shown that NaCl can significantly increase the solubility of anhydrite in a solution, thus decreasing its potential for deposition. In the Cawayan field the problem of anhydrite deposition is mainly caused by the acid fluid that corrodes the casing and permits the entry of the high-sulphate fluid. Treatment with NaCl will not solve the corrosion problem, however, it can prolong the life of the well by retarding deposition.

Figure 20 shows simulated increases in the salinity of the fluid in well CN-1 and the effect of increasing the amount of mixing fluid on anhydrite deposition.

The salinities are increased by 10, 20, 30, and 40% of the original NaCl concentration prior to mixing with different amounts of CN-1 high-sulphate downhole fluid. Results show that as the amount of NaCl is increased, the amount of anhydrite deposit is significantly decreased. The fraction of the downhole fluid required to initiate deposition is also increased.

Injection with NaCl in the acid zones during drilling is also a possibility. Instead of inducing deposition by $CaCl_2$ injection, NaCl can be pumped into the acid zones during drilling and thus significantly reduce the tendency of the high sulphate acid fluid to cause anhydrite deposition when it mixes with the hotter calcium-rich geothermal brine.

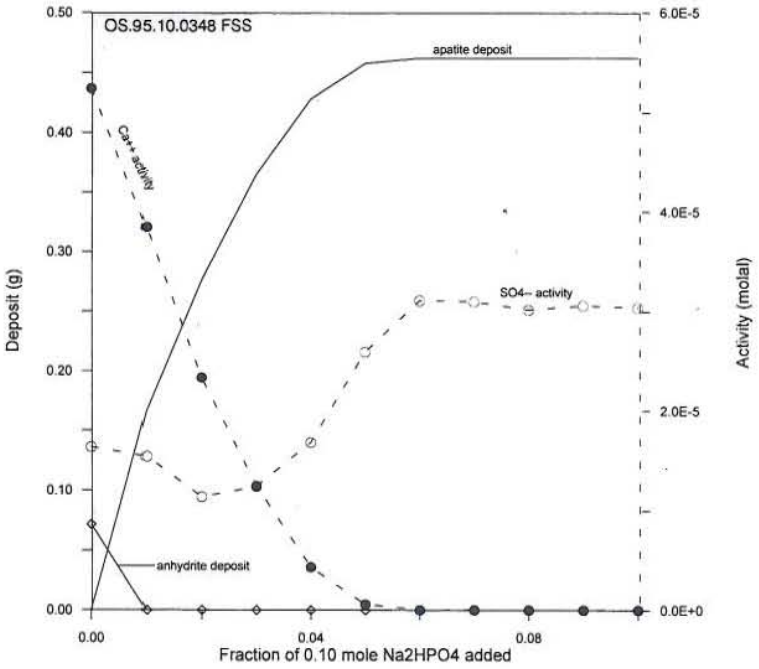

FIGURE 21: Effect of Na_2HPO_4 addition on CN-1 fluid, supersaturated with anhydrite at 270°C

Addition of Na_2HPO_4 also indicated some promising results (Figure 21). Titration of CN-1 fluid supersaturated with anhydrite, with 0.10 mole of Na_2HPO_4 resulted in abrupt undersaturation with respect to anhydrite at a fraction of 0.02. Na_2HPO_4 significantly reduces the activity of calcium that favours the association with the phosphate ions to form apatite, $Ca_3(PO_4)_2CaCl_2$. However, as a result of this reaction, deposition of apatite may take place as indicated by the simulation run.

9.2 pH reduction (acid injection)

Acid treatment is also a possible method of control. Although the main cause of deposition in Cawayan wells is acid fluid, the simulation runs have shown that the fraction of this acid fluid necessary for deposition is so small that it does not significantly affect the pH of the solution. Results of mixing simulation in CN-1 show that from an original downhole pH of 6.61, the mixed fluid pH decreased to only 5.62 after a 0.10 fraction of the acid fluid had been added

The effect of acidification has been simulated using CN-1 fluids mixed with 0.05 and 0.10 fractions of acid high-sulphate downhole water, titrated with 0.001 to 0.01 fractions of 0.01 mole of HCl after deposition has taken place. Figure 22 shows the

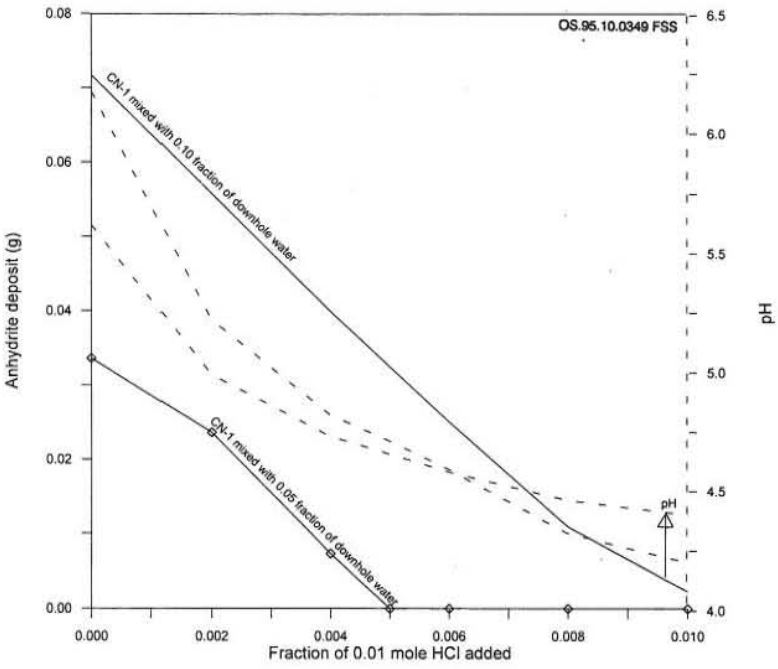

FIGURE 22: Effect of addition of 0.01 mole HCl on anhydrite deposition of CN-1 production fluid mixed with 0.05 and 0.10 fractions of high-sulphate acid downhole fluid, at 270°C

results of the simulation runs. At the assumed 0.05 fraction of downhole water, all anhydrite deposit was successfully dissolved by a 0.005 mole fraction of HCl at pH 4.71. However at a higher fraction (0.10) of high-sulphate fluid mixed with the brine, the amount of HCl needed to approach zero deposition is about 0.01 and this will reduce the pH to 4.40. The calculated downhole pH at 270°C can also decrease significantly at lower temperatures as more bisulphate ions dissociate. But acid addition can be regulated, and although deposition is not totally eliminated, it can be significantly reduced.

9.3 Synthetic chemical additives

The effect of synthetic chemical additives on the morphology of calcium sulphate precipitated from seawater at 120-150°C has been investigated by Austin, et al. (1975). The results show that additives can displace SO_4^{2-} and attach themselves to the Ca^{2+} probably by OH^- bonding on the growth surface; identified effective additives contain PO_3H^- and CO_2H. This experiment was however, conducted at relatively low temperatures.

Experimental studies for possible application in oil fields by Vetter (1972) showed that phosphonates can be effective inhibitors of anhydrite deposition at temperatures of about 350°F (177°C). No data however were available for higher temperatures. Other possible synthetic chemical additives are the NADAR Dispersants manufactured commercially by Nadar Chimica. These additives have mainly dispersant action and some complexing activity towards calcium salts in saline environment (A. Prinetti, pers. comm.)

10. SUMMARY AND CONCLUSIONS

The anhydrite deposition in Cawayan wells is basically controlled by three factors: high-sulphate acid fluid, calcium-rich geothermal brine, and a high temperature of mixing. Mixing simulations and geochemical evidence suggest that the anhydrite deposit is an end-product of mixing between high-sulphate acid fluid and calcium-rich geothermal brine. Geochemical parameters such as sulphate, calcium, magnesium, chloride, and silica are effective indicators of deposition. The speciation programmes WATCH and SOLVEQ can be used to monitor the anhydrite saturation of the fluids.

The reaction path programme CHILLER can be an effective tool in predicting and possibly quantifying the rate and amount of anhydrite deposition. Preliminary results of simulation runs suggest that in the complex geochemical matrix of the Cawayan well fluids, the behaviour of calcium and sulphate species can be manipulated by the addition of chemicals in such a way that the tendency for anhydrite deposition can be significantly reduced. Possible inhibitors screened by simulations include NaCl, Na_2HPO_4, and HCl. However, as mentioned earlier, there are always limitations to chemical equilibrium computations; one of which is "kinetic barriers" (Nordstrom and Munoz, 1986). Other factors in deposition processes which may not be simulated by reaction path programmes include the effect of fluid velocity, thermal stability of some chemical inhibitors, nucleation and crystal formation, and adherence of deposits. Therefore, pilot scale experimental studies are necessary for validation.

ACKNOWLEDGEMENTS

I wish to convey my sincerest thanks to the government of Iceland, the United Nations University, PNOC-EDC, Dr. Ingvar Fridleifsson, Lúdvík Georgsson, Súsanna and Margrét Westlund, my adviser Dr. Halldór Ármannsson, Dr. Stefán Arnórsson, the Orkustofnun lecturers and staff, and the UNU fellows of 1995.

REFERENCES

Arnórsson, S., Sigurdsson, S., and Svavarsson, H., 1982: The chemistry of geothermal waters in Iceland I. Calculation of aqueous speciation from 0° to 370°C. *Geochim. Cosmochim. Acta, 46,* 1513-1532.

Austin, A.E., Miller, J.F., Vaughan, D.A., and Kircher, J.F., 1975: Chemical additives for calcium sulphate control. *Desalination, 16,* 345-357.

Bjarnason, J.Ö., 1994: *The speciation programme WATCH, version 2.1.* Orkustofnun, Reykjavík, 7 pp.

Blount, C.W., and Dickson, F.W., 1969: The solubility of anhydrite ($CaSO_4$) in NaCl-H_2O from 100 to 450°C and 1 to 1000 bars. *Geochim. Cosmochim. Acta, 33,* 227-245.

Dickson, F.W., Blount, C.W., and Tunell, G., 1963: Use of hydrothermal solution equipment to determine the solubility of anhydrite in water from 100°C to 275°C and from 1 bar to 1000 bars pressure. *Am. J. Sci., 261,* 61-78.

Fragata, J.F., 1991: *Well CN-3D geology report.* PNOC-EDC, Philippines, internal report, 26 pp.

Fragata, J.F., 1994: *Well CN-4D geology report.* PNOC-EDC, Philippines, internal report, 17 pp.

Helgeson, H.C., 1969: Thermodynamic of complex dissociation in aqueous solution at elevated temperatures and pressures. *Amer. J. Sci., 267,* 729-804.

KRTA, 1983: *Summary of calcium sulphate solubility, controls and determination.* PNOC-EDC, Philippines, internal report, 53 pp.

KRTA, 1985: *Acid sulphate fluids in the Bacon-Manito central reservoir.* PNOC-EDC, Philippines, internal report.

Nordstrom, D.K., and Munoz, J.L., 1986: *Geochemical Thermodynamics.* Blackwell Scientific Publications, Palo Alto, Ca., 477 pp.

PNOC-EDC, 1989: *Bacman II resource assessment.* PNOC-EDC, Philippines, internal report 21 pp.

Ramos, S.G., 1991: *Petrology of well CN-2RD.* PNOC-EDC, Philippines, internal report, 15 pp.

Reed, M.H., and Spycher, N.F., 1990: *SOLTHERM: Data base for equilibrium constants for aqueous - mineral-gas equilibria.* University of Oregon, Eugene, Oregon, 47 pp.

See, F.S., 1991: *Geochemistry of well CN-2RD.* PNOC-EDC, Philippines, internal report.

Solis, R.P., 1988: *Chemical signatures of the acidic fluids in the production wells of Bacon-Manito geothermal project.* PNOC-EDC, Philippines, internal report.

Solis, R.P., Cabel, A.C., See, F.S., Candelaria, M.N.R., Buenviaje, M.M., and Garcia, S.E., 1994: *Bacon-Manito geothermal production field pre-exploitation baseline geochemistry data.* PNOC-EDC, Philippines, internal report.

Spycher, N.F., and Reed, M.H., 1990: *User's guide for SOLVEQ: A computer program for computing aqueous-mineral-gas equilibria (revised preliminary edition).* University of Oregon, Eugene, Oregon, 37 pp.

Spycher, N.F., and Reed, M.H., 1992: *User's guide for CHILLER: A program for computing water-rock reactions, boiling, mixing, and other reaction processes in aqueous-mineral-gas systems*. University of Oregon, Eugene, Oregon, 68 pp.

Vetter, O.J., 1972: An evaluation of scale of inhibitors. *J. Pet. Chem., Aug. 1972,* 997-1008.

Vetter, O.J., and Phillips, R.C., 1970: Prediction of deposition of calcium sulphate scale under downhole conditions. *J. Pet. Tech., Oct. 1970,* 1299-1308.

Yeatts, L.B., and Marshall, W.L., 1969: Apparent invariance of activity coefficients of calcium sulphate at constant ionic strength and temperature in the system $CaSO_4$-Na_2SO_4-$NaNO_3$-H_2O to the critical temperature of water. *Association Equilibria, J. Phys. Chem., 73,* 81-92.

APPENDIX I: Formulas used for calculating anhydrite solubility

1. Arnórsson et al., 1982:

$$\log K = 6.20 - 0.0229\,T - \frac{1217}{T} \qquad (°K)$$

2. Yeatts and Marshall, 1969, for solid-ion equilibrium:

$$\log K_{isp} = -133.207 + 53.5472 \log T + \frac{3569.6}{T} - 0.0520925\,T \qquad (°K)$$

3. Blount and Dickson, 1969:

$$\log m_e = -2.917 - 0.02314\,t + 0.001179\,P + 6.02\times10^{-9}\,P\,t^2 - 2.07\times10^{-7}\,P^2$$

where m is solubility of anhydrite in molal, t is temperature in °C, P is pressure in bars.

4. Reed and Spycher, 1990, general equation form for all aqeous species, gases, and minerals that are incorporated in the SOLVEQ programme:

$$\log K(T) = A + B\,T + C\,T^2 + D\,T^3 + E\,T^4 \qquad (T \text{ in } °C)$$

where A, B, C, D, E are the regression coefficients.

For *anhydrite* = $1.0\,Ca^{++} + 1.0\,SO_4^{2-}$

A = -4.046801, B = -0.0065771, C = -0.10075×10^{-3}, D = -0.45922×10^{-6}, E = -0.92941×10^{-9}

log K values are:

-4.265 at 25°C,	-4.580 at 50°C,	-5.345 at 100°C,	-6.216 at 150°C,
-7.213 at 200°C,	-8.439 at 250°C,	-10.218 at 300°C,	-14.022 at 350°C

APPENDIX II: Samples of CHIILER run input data and ouput

CN-1 Production Fluid (09-29-81) MIX WITH CN-1 Downhole fluid (09-04-89)
CHILLER RUN

```
< erpc >< ph  >< pfluid >< temp >< tempc ><volbox-1><rhofresh>< rhoroc >
.1000E-11   .00000 55.00000 270.00000  270.00000   .00000   .00000   .00000

<   sinc  ><   slim  ><  totmix  >
 0.010000000     0.1000000    .000000000

< enth >< senth >< denth >< totwat >< solmin ><  rm  >< aqgrm >< suprnt >
  .00000   .00000   .00000 90.00000 .0000E+00   .00000 999.08765 .1000E-19

-----  c ifra ipun nloo iste lims looc ient itre idea ipsa incr incp mins neut
  0  3  0  2  70  0  1  0  0  0  0  1  0  0  0  0
```

saq>	< name >	< mtot ><	mtry ><	gamma >	< comtot >
1	H+	.300600000E-04	.408183988E-06	.5104	.2138E-02
2	H2O	.984667000E+00	.100000000E+01	.9929	.995316E+00
3	Cl-	.235011443E+00	.215929676E+00	.4902	.4616E-01
4	SO4--	.270700000E-03	.921174811E-04	.0811	.9202E-02
5	HCO3-	.289600000E-03	.239437435E-04	.5049	.1120E-02
6	HS-	.524700000E-05	.143917094E-05	.4918	.000000E+00
7	SiO2(aq)	.144000000E-01	.773939953E-02	1.0000	.9521E-02
9	Ca++	.441600000E-02	.827521482E-03	.0726	.2246E-03
10	Mg++	.781500000E-05	.228567365E-07	.0641	.3866E-03
12	K+	.229700000E-01	.217242575E-01	.5095	.3683E-02
13	Na+	.204000000E+00	.190058424E+00	.4918	.5655E-01
11	Fe+	.000000000E+00	.000000000E+00		.1046E-02

```
< min  >  < mintry >

<nomox >  <  wtpc  ><ppm?
```

<supnam>	antigori	Fe-actin
diopside	anthophy	enstatit
quartz	chrysoti	andradit
chalcedo	cristoba	cristo-a
talc	wollasto	hedenber
rhodonit	tremolit	<dontfr>

CN-1 9-29-81 MIX WITH CN-1 DOWNHOLE 9-4-89
CHILLER

SPECIES	NO.	CHARGE	TOT.MOLES	MTRY	GAMMA	MIXING SOLUTION
H+	1	1.	.30060E-04	.40818E-06	.5104	.21380000E-02
H2O	2	0.	.54657E+02	.10000E+01	.9929	.55248250E+02
Cl-	3	-1.	.23501E+00	.21593E+00	.4902	.46160000E-01
SO4--	4	-2.	.27070E-03	.92117E-04	.0811	.92020000E-02
HCO3-	5	-1.	.28960E-03	.23944E-04	.5049	.11200000E-02
HS-	6	-1.	.52470E-05	.14392E-05	.4918	.00000000E+00
SiO2(aq)	7	0.	.14400E-01	.77394E-02	1.0000	.95210000E-02
Ca++	8	2.	.44160E-02	.82752E-03	.0726	.22460000E-03
Mg++	9	2.	.78150E-05	.22857E-07	.0641	.38660000E-03
K+	10	1.	.22970E-01	.21724E-01	.5095	.36830000E-02
Na+	11	1.	.20400E+00	.19006E+00	.4918	.56550000E-01
Fe++	12	2.	.00000E+00	.10000E-09	1.0000	.10460000E-02

```
   CHARGE BALANCE FOR TOTAL MOLES = -.27755576E-16
     MAX. DIFFERENCE ALLOWED =  .235011446-04
  CHARGE BALANCE FOR THE MIXING SOLUTION =  .1408E-05
     MAX. DIFFERENCE ALLOWED =  .2350E-04

  THE FOLLOWING PARAMETERS WERE GIVEN:
    ERPC  = .1000E-11  PH     =     .0000   Pfluid =   55.0000
    SLIM  = .10000E+00   TEMP   =  270.0000   SINC   = .1000E-01
    TEMPC =  270.0000  TOTMIX= .00000E+00    ENTH   =     .0000
    SENTH =     .0000  DENTH  =     .0000   TOTWAT =   90.0000
    SOLMIN= .0000E+00  RM     =     .0000   AQGRM  =  999.0877
    SUPRNT= .1000E-19  Vbox-1 =     .0000   Rhofre =     .0000
    Rhoroc=     .0000

  THE FOLLOWING OPTIONS WERE SELECTED:
    C     =   3  IFRAC =   0  IPUNCH =   2  NLOOP =   70
    ISTEP =   0  LIMSOL =   1  LOOC  =   0  IENTH =    0
    ITREF =   0  IDEAL  =   0  IPSAT =   1  INCREM=    0
    INCP  =   0  MINSOL =   0  NEUT  =   0

    GIVEN PRESSURE GRID.   1 T-P POINTS READ

OF THE DERIVED SPECIES LISTED BELOW, ONLY THOSE WITH
MOLALITIES ABOVE  .1000E-19 WILL APPEAR ON THE OUTPUT
```

SPECIES	NO.	CHARGE	LOG K(DISS)	SPECIES	NO.	CHARGE	LOG K(DISS)
CaCl+	13	1.	-2.3828	FeSO4	36	0.	-6.5449
CaCl2	14	0.	-2.9515	H2 aq.	37	0.	6.8012
CaCO3	15	0.	5.2801	KCl	38	0.	-.1197

CaHCO3+	16	1.	-2.3957	KHSO4	39	0.	-6.5465
CaOH+	17	1.	7.1977	KSO4-	40	-1.	-2.5532
CaSO4	18	0.	-4.0917	MgCl+	41	1.	-2.3828
CH4 aq.	19	0.	5.8684	MgCO3	42	0.	5.7459
HCl	20	0.	-.7292	MgHCO3+	43	1.	-2.9719
CO3--	21	-2.	11.5147	MgOH+	44	1.	5.8736
H2CO3	22	0.	-8.0493	MgSO4	45	0.	-4.8303
FeCl+	23	1.	-2.6312	NaCl	46	0.	-.2349
FeCl2	24	0.	-2.0800	NaCO3-	47	-1.	9.3584
Fe3+	25	3.	8.3179	NaHCO3	48	0.	-.5695
FeCl++	26	2.	2.3526	NaHS	49	0.	-.5695
FeCl2+	27	1.	5.8700	NaOH	50	0.	10.8546
FeCl3	28	0.	-.0486	NaSO4-	51	-1.	-1.9122
FeCl4-	29	-1.	.6149	O2 aq.	52	0.	32.6587
FeOH+	30	1.	6.9461	OH-	53	-1.	11.1205
Fe(OH)2	31	0.	12.6124	S--	54	-2.	15.0210
Fe(OH)3	32	0.	11.4134	H2S aq.	55	0.	-7.2937
Fe(OH)3-	33	-1.	21.5608	HSO4-	56	-1.	-5.7117
Fe(OH)4-	34	-1.	19.5640	H2SiO4--	57	-2.	21.4675
FeSO4+	35	1.	-1.1697	H3SiO4-	58	-1.	8.9429

FOR MIXED GASES (JSOLS=6), LOG K(HYDROL) = LOG (K*P)

MINERAL	NO.	LOG K(HYDROL)	TRIAL MOLES	MINERAL	NO.	LOG K(HYDROL)	TRIAL MOLES
H2O gas	1	.082	.0000E+00	greenali	26	14.677	.0000E+00
CO2 gas	2	-8.107	.0000E+00	gruneri*	27	16.255	.0000E+00
CH4 gas	3	4.944	.0000E+00	gypsum	28	-7.547	.0000E+00
H2 gas	4	5.870	.0000E+00	halite	29	.704	.0000E+00
H2S gas	5	-7.484	.0000E+00	hematite	30	5.429	.0000E+00
HCl gas	6	.861	.0000E+00	huntite	31	-8.180	.0000E+00
SO2 gas	7	-6.359	.0000E+00	kerolite	32	12.373	.0000E+00
S2 gas	8	-12.882	.0000E+00	lime	33	17.478	.0000E+00
O2 gas	9	30.129	.0000E+00	magnesit	34	-2.440	.0000E+00
akermani	10	21.648	.0000E+00	magn-hyd	35	4.527	.0000E+00
anhydrit	11	-9.068	.0000E+00	magnetit	36	8.979	.0000E+00
aragonit	12	-1.407	.0000E+00	merwinit	37	33.817	.0000E+00
artinite	13	9.341	.0000E+00	monticel	38	13.939	.0000E+00
brucite	14	8.034	.0000E+00	nesqueho	39	13.280	.0000E+00
calcite	15	-1.580	.0000E+00	periclas	40	9.779	.0000E+00
camin625	16	-4.471	.0000E+00	portland	41	12.423	.0000E+00
camin75	17	-2.726	.0000E+00	pyrite	42	-20.151	.0000E+00
cristo-b	18	-1.695	.0000E+00	pyrrhoti	43	-6.354	.0000E+00
dolomite	19	-4.838	.0000E+00	pyrrhot!	44	-6.350	.0000E+00
dolo-ord	20	-4.839	.0000E+00	S native	45	-8.904	.0000E+00
dolo-dis	21	-4.263	.0000E+00	sepiolit	46	16.796	.0000E+00
fayalite	22	6.564	.0000E+00	siderite	47	-4.154	.0000E+00
ferreil	23	2.246	.0000E+00	silic-am	48	-1.648	.0000E+00
forsteri	24	11.508	.0000E+00	sylvite	49	.831	.0000E+00
graphite	25	-2.310	.0000E+00	minneso*	50	3.208	.0000E+00

```
     THE FOLLOWING MINERALS AND/OR GASES WITH IDENTICAL
       INDEX ARE IN SOLID SOLUTION:

       H2O gas        6
       CO2 gas        6
       CH4 gas        6
       H2 gas         6
       H2S gas        6
       HCl gas        6
       SO2 gas        6
       S2 gas         6
       minneso*       7
*************************************************************************
CN-1 9-29-81 MIX WITH CN-1 DOWNHOLE 9-4-89
CHILLER
*************************************************************************

 NUMBER OF LOOPS USED =  13    LOOP LIMIT =  70

    CHARGE BALANCE FOR TOTAL MOLES = -.2755576E-16
     MAX. DIFFERENCE ALLOWED =  .23501144E-04

TEMPERATURE=270.0000 C.  P(FLUID)= 55.00000 BARS  MIXER FRACTION=      .0000000
 WATER:  MOLES LIQ. =   54.6568   KG. LIQ.  =  .9847E+00
         MOLES TOTAL=   54.6571   KG. TOTAL=  .9847  ACTIVITY= .9929
        STOICHIOMETRIC IONIC STRENGTH=.2442728E+00   OSMOTIC COEF.=  .8230

 TRUE IONIC STRENGTH=.2174301E+00

                              LOG                          LOG              LOG
  SPECIES(N)    MOLALITY    MOLALITY     ACTIVITY       ACTIVITY    GAMMA    GAMMA

  1 H+         .47577E-06   -6.3226   .24280E-06    -6.6147  .51033E+00   -.2922
  2 H2O                                .99293E+00     -.0031  .99292E+00   -.0031
  3 Cl-        .21592E+00     -.6657  .10583E+00     -.9754  .49012E+00   -.3097
  4 SO4--      .92000E-04   -4.0362  .74553E-05    -5.1275  .81037E-01   -1.0913
  5 HCO3-      .20867E-04   -4.6805  .10535E-04    -4.9774  .50486E+00   -.2968
  6 HS-        .13225E-05   -5.8786  .65032E-06    -6.1869  .49172E+00   -.3083
  7 SiO2(aq)   .14487E-01   -1.8390  .14487E-01    -1.8390  .10000E+01    .0000
  8 Ca++       .83022E-03   -3.0808  .60260E-04    -4.2200  .72583E-01   -1.1392
  9 Mg++       .16131E-05   -5.7923  .10332E-06    -6.9858  .64047E-01   -1.1935
 10 K+         .21725E-01   -1.6630  .11067E-01    -1.9560  .50941E+00   -.2925
 11 Na+        .19007E+00     -.7211  .93468E-01    -1.0293  .49177E+00   -.3082
 12 Fe++      .70395E-23  -23.1525  .46535E-24   -24.3322  .66106E-01   -1.1798
 13 CaCl+     .30118E-02   -2.5212  .15398E-02    -2.8125  .51125E+00   -.2914
 14 CaCl2     .60360E-03   -3.2193  .60360E-03    -3.2193  .10000E+01    .0000
 15 CaCO3     .13719E-07   -7.8627  .13719E-07    -7.8627  .10000E+01    .0000
 16 CaHCO3+   .30883E-05   -5.5103  .15789E-05    -5.8016  .51125E+00   -.2914
 17 CaOH+     .30572E-04   -4.5147  .15630E-04    -4.8060  .51125E+00   -.2914
 18 CaSO4     .55492E-05   -5.2558  .55492E-05    -5.2558  .10000E+01    .0000
 19 CH4 aq.   .11488E-11  -11.9398  .12353E-11   -11.9082  .10754E+01    .0316
 20 HCl       .13774E-06   -6.8609  .13774E-06    -6.8609  .10000E+01    .0000
 21 CO3--     .17206E-08   -8.7643  .13264E-09    -9.8773  .77088E-01   -1.1130
 22 H2CO3     .26648E-03   -3.5743  .28657E-03    -3.5428  .10754E+01    .0316
 23 H2 aq.    .35725E-05   -5.4470  .38418E-05    -5.4155  .10754E+01    .0316
 24 KCl       .15427E-02   -2.8117  .15427E-02    -2.8117  .10000E+01    .0000
 25 KHSO4     .70502E-07   -7.1518  .70502E-07    -7.1518  .10000E+01    .0000
 26 KSO4-     .60173E-04   -4.2206  .29492E-04    -4.5303  .49012E+00   -.3097
 27 MgCl+     .51637E-05   -5.2870  .26480E-05    -5.5784  .51125E+00   -.2914
 28 MgCO3     .80469E-11  -11.0944  .80469E-11   -11.0944  .10000E+01    .0000
 29 MgHCO3+   .19957E-08   -8.6999  .10203E-08    -8.9913  .51125E+00   -.2914
 30 MgOH+     .11057E-05   -5.9563  .56531E-06    -6.2477  .51125E+00   -.2914
 31 MgSO4     .52108E-07   -7.2831  .52108E-07    -7.2831  .10000E+01    .0000
 32 NaCl      .16987E-01   -1.7699  .16987E-01    -1.7699  .10000E+01    .0000
 33 NaCO3-    .36256E-08   -8.4406  .17770E-08    -8.7503  .49012E+00   -.3097
 34 NaHCO3    .36543E-05   -5.4372  .36543E-05    -5.4372  .10000E+01    .0000
 35 NaHS      .22558E-06   -6.6467  .22558E-06    -6.6467  .10000E+01    .0000
 36 NaOH      .53419E-05   -5.2723  .53419E-05    -5.2723  .10000E+01    .0000
 37 NaSO4-    .11416E-03   -3.9349  .56935E-04    -4.2446  .49012E+00   -.3097
 38 OH-       .66688E-04   -4.1773  .30984E-04    -4.5089  .46600E+00   -.3316
 39 S--       .33102E-13  -13.4802  .25518E-14   -14.5932  .77088E-01   -1.1130
 40 H2S aq.   .28875E-05   -5.5395  .31051E-05    -5.5079  .10754E+01    .0316
 41 HSO4-     .18014E-05   -5.7444  .93203E-06    -6.0306  .51740E+00   -.2862
 42 H2SiO4--  .10712E-08   -8.9701  .42577E-10   -10.0831  .77088E-01   -1.1130
 43 H3SiO4-   .13690E-03   -3.8636  .67099E-04    -4.1733  .49012E+00   -.3097

 CHARGE BALANCE FOR ALL SPECIES =  .6481E-16



 TOTAL FRACTION OF MIXING SOLUTION ADDED:      .0000000

 Solid products produced:  Mass:      .000000 grams    Volume:      .000000 CM3
    Warning, mineral volume may be in error because some mineral densities
    were not supplied in SOLTHERM.  See mineral list at top of output.
```

```
 GAS COMPOSITION AT SATURATION (  4 ITERATIONS)
 ----------------------------------------------

 TEMPERATURE:      270.0000 DEG.C.
 SAT. PRESSURE:     54.3250 BARS

   GAS          MOLE FRAC.      PHI       FUGACITY      PARTIAL P. (BARS)

 H2O gas       .9996E+00     .8333     .4525E+02      .5430E+02
 CO2 gas       .3402E-03     .9806     .1812E-01      .1848E-01
 CH4 gas       .8949E-11    1.1751     .5713E-09      .4862E-09
 H2 gas        .3256E-04    1.0199     .1804E-02      .1769E-02
 H2S gas       .5209E-05     .9350     .2646E-03      .2830E-03
 HCl gas       .3587E-08    1.0000     .1948E-06      .1948E-06
 SO2 gas       .2510E-10    1.0000     .1363E-08      .1363E-08
 S2 gas        .3255E-15    1.0000     .1768E-13      .1768E-13

 NON-IDEAL MIXING WITH H2O, CO2, CH4 GASES

*************************************************************************

  The following gases and minerals are presently EXCLUDED from matrix
 (Note that gases and minerals with log(Q/K) less than -5 are not listed below)

 GAS OR MINERAL  LOG K   LOG Q  LOG(Q/K)  LOG(Q/K)/S  AFFINITY  LOG FUGACITY

  1 H2O gas       .08     .00     -.08       -.085   .21061E+03     1.656
  2 CO2 gas     -8.11  -11.59    -3.48      -1.161   .86558E+04    -1.742
  3 CH4 gas      4.94   -6.04   -10.98      -2.746   .27303E+05    -9.243
  4 H2 gas       5.87    1.39    -4.48      -2.562   .11147E+05    -2.744
  5 H2S gas     -7.48  -12.80    -5.32      -2.659   .13219E+05    -3.577
  6 HCl gas       .86   -7.59    -8.45      -4.225   .21007E+05    -6.710
  7 SO2 gas     -6.36  -16.97   -10.61      -2.828   .26364E+05    -8.865
  8 S2 gas     -12.88  -28.37   -15.49      -2.384   .38512E+05   -13.752
  9 O2 gas      30.13   -2.78   -32.91     -21.938   .81800E+05   -32.907
 10 akermani    21.67   20.58    -1.09       -.078   .27155E+04
 11 anhydrit    -9.07   -9.35     -.28       -.140   .69546E+03
 12 aragonit    -1.41   -2.58    -1.18       -.192   .29225E+04
 14 brucite      8.03    6.24    -1.80       -.359   .44651E+04
 15 calcite     -1.58   -2.58    -1.00       -.334   .24929E+04
 18 cristo-b    -1.69   -1.84     -.14       -.144   .35864E+03
 19 dolomite    -4.84   -7.93    -3.09       -.516   .76888E+04
 20 dolo-ord    -4.84   -7.93    -3.09       -.515   .76863E+04
 21 dolo-dis    -4.26   -7.93    -3.67       -.611   .91183E+04
 24 forsteri    11.51   10.64     -.87       -.096   .21530E+04
 28 gypsum      -7.55   -9.35    -1.81       -.452   .44911E+04
 29 halite        .70   -2.00    -2.71      -1.354   .67335E+04
 32 kerolite    12.37   11.35    -1.02       -.051   .25335E+04
 34 magnesit    -2.44   -5.35    -2.91       -.969   .72298E+04
 37 merwinit    33.82   29.58    -4.23       -.235   .10527E+05
 38 monticel    13.94   13.41     -.53       -.059   .13201E+04
 40 periclas     9.78    6.24    -3.54       -.884   .87947E+04
 41 portland    12.42    9.00    -3.42       -.684   .85018E+04
 46 sepiolit    16.80   13.91    -2.89       -.100   .71821E+04
 48 silic-am    -1.64   -1.84     -.20       -.199   .49359E+03
 49 sylvite       .83   -2.93    -3.76      -1.881   .93537E+04

 Calculations done for   270.0000 DEG.C.;      55.0000 BARS

    MIXER FRACTION:      .000000

                          TEMPERATURE   STOC.IONIC STRENGTH   HEAT PER MOLE

    ACTUAL SOLUTION:        270.000          .24427E+00          65.722
    MIXING SOLUTION:        270.000          .00000E+00            .000

    FRACT. OF MIXING SOLUTION ADDED:     .010000
       BITMOL= .5525E+00  OLDMOL= .5490E+02

    NEW HEAT:     65.722     NEW TEMPERATURE: 270.000

    NEW MIXER FRACTION:      .010000
    RESULTING TEMPERATURE: 270.000DEG.C.

    SOLIDS AND GASES CARRIED

    CHARGE BALANCE CHECK AFTER FRACTIONATION OR TITRATION : TBAL =  .1400E-07
1
*************************************************************************
CN-1 9-29-81 MIX WITH CN-1 DOWNHOLE 9-4-89
CHILLER
*************************************************************************

 NUMBER OF LOOPS USED =  10    LOOP LIMIT =  70

    CHARGE BALANCE FOR TOTAL MOLES = .14000000E-07
     MAX. DIFFERENCE ALLOWED =  .23547304E-04
```

APPENDIX III: Sample calculation of anhydrite saturation (from CN-3D data, 10-11-90)

Webre conc. @ SP=7.3 bars / H_d= 1232 kJ/kg:	SO_4^{2-} = 25.0 mg/kg	Ca^{2+} = 174 mg/kg
Activity coefficients at 273°C:	SO_4^{2-} = 0.09	Ca^{2+} = 0.132
Species in deep water:	SO_4^{2-} = 6.52 mg/kg	Ca^{2+} = 129.9 mg/kg
Activity in Deep Water:	= γ * ...	

$m\ SO_4^{2-}$ = (6.52 mg/kg)/(96000mg/mole) = 6.792×10^{-5} mole/kg

$a\ SO_4^{2-}$ = 0.09*6.792×10^{-5} mole/kg = 6.112×10^{-6} mole/kg

$m\ Ca^{2+}$ = (129.9 mg/kg)/(40080 mg/mole) = 3.184×10^{-3} mole/kg

$a\ Ca^{2+}$ = 0.132*3.241×10^{-3} mole/kg = 4.203×10^{-4} mole/kg

$Q_{CaSO4} = a_{SO4--} * a_{Ca++} = 6.112 \times 10^{-6} * 4.203 \times 10^{-4} = 2.569 \times 10^{-9}$

$log\ Q_{CaSO4}$ = -8.590

$log\ K_{CaSO4}$ = -8.582 at 273 °C (calculated from thermodynamic data)

$log\ (Q/K)$ = -8.590 -(-8.528) = -0.008

thus this fluid is very slightly undersaturated or in near equilibrium with anhydrite since the log ratio is practically zero ($log\ Q = log\ K$)